Published in final edited form as:

J Phys Chem Ref Data. 2017 June ; 46(2): . doi:10.1063/1.4983027.

Correlations for the Viscosity and Thermal Conductivity of Ethyl Fluoride (R161)[a)]

Ch. M. Tsolakidou[1], **M. J. Assael**[1,b], **M. L. Huber**[2], and **R. A. Perkins**[2]

[1]Laboratory of Thermophysical Properties and Environmental Processes, Chemical Engineering Department, Aristotle University, Thessaloniki 54636, Greece

[2]Applied Chemicals and Materials Division, National Institute of Standards and Technology, 325 Broadway, Boulder, CO 80305, USA

Abstract

This paper presents new wide-ranging correlations for the viscosity and thermal conductivity of ethyl fluoride (R161) based on critically evaluated experimental data. The correlations are designed to be used with a recently published equation of state that is valid from 130 K to 450 K, at pressures up to 100 MPa. The estimated uncertainty at a 95% confidence level is 2% for the viscosity of low-density gas (pressures below 0.5 MPa), and 3% for the viscosity of the liquid over the temperature range from 243 K to 363 K at pressures up to 30 MPa. The estimated uncertainty is 3% for the thermal conductivity of the low-density gas, and 3% for the liquid over the temperature range from 234 K to 374 K at pressures up to 20 MPa. Both correlations may be used over the full range of the equation of state, but the uncertainties will be larger, especially in the critical region.

Keywords

critical phenomena; ethyl fluoride; R161; thermal conductivity; transport properties; viscosity

1. Introduction

In a series of recent papers, new reference correlations for the thermal conductivity of normal- and parahydrogen,[1] water,[2] SF_6,[3] carbon dioxide,[4] toluene,[5] benzene,[6] *n*-hexane,[7] cyclohexane,[8] *n*-heptane,[9] methanol,[10] ethanol,[11] ethene and propene,[12] and ortho-xylene, meta-xylene, para-xylene, and ethylbenzene,[13] as well as for the viscosity of water,[14] *n*-hexane,[15] *n*-heptane,[16] benzene[17] and toluene,[18] covering a wide range of conditions of temperature and pressure, were reported. The work was also extended to refrigerants; thus reference correlations for the thermal conductivity of R245fa,[19] and for the viscosity of R1234yf and R1234ze(E),[20] and R245fa,[19] were reported. In this paper, the methodology adopted in the aforementioned papers is extended to developing new reference correlations for the viscosity and thermal conductivity of ethyl fluoride (R161), also called fluoroethane.

[a)]Partial contribution of NIST, not subject to copyright in the U.S.

[b]Author to whom correspondence should be addressed (assael@auth.gr).

The goal of this work is to critically assess the available literature data, and provide wide-ranging correlations for the viscosity and thermal conductivity of R161 that are valid over gas, liquid, and supercritical states, and that incorporate densities provided by the recently published Helmholtz equation of state of Qi *et al.*[21]

The analysis that will be described will be applied to the best available experimental data for the viscosity and thermal conductivity. Thus, a prerequisite to the analysis is a critical assessment of the experimental data. For this purpose, two categories of experimental data are defined: primary data, employed in the development of the correlation, and secondary data, used simply for comparison purposes. According to the recommendation adopted by the Subcommittee on Transport Properties (now known as The International Association for Transport Properties) of the International Union of Pure and Applied Chemistry, the primary data are identified by a well-established set of criteria.[22] These criteria have been successfully employed to establish standard reference values for the viscosity and thermal conductivity of fluids over wide ranges of conditions, with uncertainties in the range of 1%. However, in many cases, such a narrow definition unacceptably limits the range of the data representation. Consequently, within the primary data set, it is also necessary to include results that extend over a wide range of conditions, albeit with a poorer accuracy, provided they are consistent with other more accurate data or with theory. In all cases, the accuracy claimed for the final recommended data must reflect the estimated uncertainty in the primary information.

2. Viscosity Methodology

The viscosity η can be expressed[15–20] as the sum of four independent contributions, as

$$\eta(\rho,T)=\eta_0(T)+\eta_1(T)\rho+\Delta\eta(\rho,T)+\Delta\eta_c(\rho,T), \quad (1)$$

where ρ is the molar density, T is the absolute temperature, and the first term, $\eta_0(T) = \eta(0,T)$, is the contribution to the viscosity in the dilute-gas limit, where only two-body molecular interactions occur. The linear-in-density term, $\eta_1(T)\rho$, known as the initial density dependence term, can be separately established with the development of the Rainwater-Friend theory[23–25] for the transport properties of moderately dense gases. The critical enhancement term, $\Delta\eta_c(\rho,T)$, arises from the long-range density fluctuations that occur in a fluid near its critical point, which contribute to divergence of the viscosity at the critical point. Finally, the term $\Delta\eta(\rho,T)$, the residual term, represents the contribution of all other effects to the viscosity of the fluid at elevated densities including many-body collisions, molecular-velocity correlations, and collisional transfer.

The identification of these four separate contributions to the viscosity and to transport properties in general is useful because it is possible, to some extent, to treat $\eta_0(T)$, $\eta_1(T)$, and $\Delta\eta_c(\rho,T)$ theoretically. In addition, it is possible to derive information about both $\eta_0(T)$ and $\eta_1(T)$ from experiment. In contrast, there is little theoretical guidance concerning the residual contribution, $\Delta\eta(\rho,T)$, and therefore its evaluation is based entirely on an empirical equation obtained by fitting experimental data.

Table 1 summarizes, to the best of our knowledge, the experimental measurements[26–29] of the viscosity of R161 reported in the literature. In 2015, two viscosity measurement sets of R161 were published by researchers at Xi'an Jiaotong University. The measurements of Bi *et al.*[26] were performed along the liquid saturation line on a surface-light-scattering instrument with an uncertainty of 2%. The measurements of Meng *et al.*,[27] extending up to 30 MPa, were performed in a vibrating-wire instrument with an uncertainty of 3%. As measurements from this group have been successfully employed in many reference correlations,[18–20] they are here also considered as primary data. Lv *et al.*[28] employed an oscillating-disk viscometer for measurements in the vapor phase up to 3.8 MPa, with a quoted uncertainty of 1%. Lv *et al.*[28] required densities in their working formula to analyze their data, and they list densities along with their viscosity results. However, the densities employed over 0.5 MPa start to show large (up to 50%) deviations from the densities calculated from the recent equation of state of Qi *et al.*[21] We were unable to resolve the discrepancy, and thus measurements over 0.5 MPa (73 points) were disregarded and are not included in the primary data set. Points below 0.5 MPa were kept as primary data, since they are the only vapor-phase data available today, and at the lowest densities errors in density are not as significant. Finally, the saturated-liquid viscosity measurements of Fan *et al.*[29] obtained in a calibrated capillary viscometer with an uncertainty of 3% were also included in the primary data set. No other data, to our knowledge, are available for the viscosity of R161.

Figures 1 and 2 show the ranges of the primary measurements outlined in Table 1, and the phase boundary may be seen as well. The development of the correlation requires densities; Qi *et al.*[21] recently published an accurate, wide-ranging equation of Helmholtz-energy equation of state that is valid from the triple point up to 420 K and 100 MPa, with an uncertainty of 0.25% in density. We also adopt the values for the critical point and triple point from their equation of state; the critical temperature, T_c, and the critical density, ρ_c, are 375.25 K and 302.001 kg m^{-3}, respectively.[21] The triple-point temperature is 130.0 K.[21]

2.1. The viscosity dilute-gas limit and the initial-density dependence terms

The dilute-gas limit viscosity, $\eta_0(T)$ in μPa s, can be analyzed independently of all other contributions in Eq. (1). According to kinetic theory, the viscosity of a pure polyatomic gas may be related to an effective collision cross section, which contains all the dynamic and statistical information about the binary collision. For practical purposes, this relation is formally identical to that of monatomic gases and can be written as:[30]

$$\eta_0(T)=\frac{0.021357\sqrt{\mathrm{MT}}}{\sigma^2 S_\eta^*(T^*)}, \quad (2)$$

where $S_\eta^*=S(2000)/(\pi\sigma^2 f_n)$ is a reduced effective cross section, M is the molar mass in g mol^{-1}, σ is the length scaling parameter in nm, and f_η is a dimensionless higher-order correction factor according to Chapman and Cowling.[31, 32] In the above expression for S_η^*, $S(2000)$ is a generalized cross section that includes all of the information about the dynamics of the binary collisions that govern transport properties, and in turn are governed

by the intermolecular potential-energy surface.[30] The effective cross section is usually expressed in the functional form

$$\ln S_\eta^*(T^*)=\alpha_0+\alpha_1 \ln T^*, \quad (3)$$

$$T^*=k_B T/\varepsilon, \quad (4)$$

where T^* is the reduced temperature, ε/k_B is an energy scaling parameter in K, and k_B is Boltzmann's constant (1.380 648 52×10^{-23} J K^{-1}).

The temperature dependence of the linear-in-density coefficient of the viscosity $\eta_1(T)$ in Eq. (1) is very large at subcritical temperatures, and must be taken into account to obtain an accurate representation of the behavior of the viscosity in the vapor phase. It changes sign from positive to negative as the temperature decreases. Therefore, the viscosity along an isotherm should first decrease in the vapor phase and subsequently increase with increasing density.[30] Vogel *et al.*[33] have shown that fluids exhibit the same general behavior of the initial density dependence of viscosity, which can also be expressed by means of the second viscosity virial coefficient $B_\eta(T)$ as

$$B_\eta(T)=\frac{\eta_1(T)}{\eta_0(T)}. \quad (5)$$

The second viscosity virial coefficient can be obtained according to the theory of Rainwater and Friend[23, 24] as a function of a reduced second viscosity virial coefficient, $B_\eta^*(T^*)$ as

$$B_\eta^*(T^*)=\frac{B_\eta(T)}{N_A\sigma^3}, \quad (6)$$

where[30]

$$B_\eta^*(T^*)=\sum_{i=0}^{6} b_i (T^*)^{-0.25i}+b_7(T^*)^{-2.5}+b_8(T^*)^{-5.5}. \quad (7)$$

In the above equations, N_A is Avogadro's constant.

Eqs. (2) – (7) present a consistent scheme for the correlation of the dilute-gas limit viscosity, $\eta_0(T)$ and the initial density dependence term, $\eta_1(T)$. In the particular case of R161, the measurements of Lv *et al.*[28] at pressures below 0.5 MPa were employed in order to fit the coefficients a_i in Eq. (3) and the scaling parameters σ and ε/k_B. The values obtained are shown in Table 2. The coefficients b_i in Eq. (7) from ref.[30] are given in Table 3.

2.2. The viscosity critical enhancement term

Viscosity and thermal conductivity of pure fluids diverge at the critical point due to long-range fluctuations. The critical enhancements can be described by a theoretical crossover model originally developed by Bhattacharjee *et al.*,[34] Olchowy and Sengers[35] and modified by Luettmer-Strathmann *et al.*[36] Unlike the critical enhancement in thermal conductivity (which will be discussed in Section 3.3), the enhancement in viscosity is confined to a small region becoming relevant only at temperatures and densities very close to the critical point. For some fluids,[37, 38] the ratio $\Delta\eta_c(\rho,T)/\eta(\rho,T)$ exceeds 0.01 only within 1% of the critical temperature of the fluid. There are almost no data for the viscosity of R161 in the critical region. Hence, the critical enhancement for viscosity is considered negligible and it is not further taken into consideration in this work.

2.3. The viscosity residual term

As stated in Section 2, the residual viscosity term, $\Delta\eta(\rho,T)$, represents the contribution of all other effects to the viscosity of the fluid at elevated densities including many-body collisions, molecular-velocity correlations, and collisional transfer. Because there is little theoretical guidance concerning this term, its evaluation here is based entirely on experimentally obtained data.

The procedure adopted during this analysis used symbolic regression software[39] to fit all the primary data to the residual viscosity. Symbolic regression is a type of genetic programming that allows the exploration of arbitrary functional forms to regress data. The functional form is obtained by use of a set of operators, parameters, and variables as building blocks. Most recently this method has been used to obtain correlations for the viscosity of *n*-hexane,[15] *n*-heptane,[16] R1234yf and R1234ze(E),[20] and R245fa.[19] In the present work, we restricted the operators to the set (+,−,*,/) and the operands (constant, T_r, ρ_r), with $T_r = T/T_c$ and $\rho_r = \rho/\rho_c$. Various choices of a scaling factor for density were tested, but the best results were obtained using the critical density. In addition, we found the best results when we adopted a form suggested from the hard-sphere model employed by Assael *et al.*,[40] $\Delta\eta(\rho_r,T_r)=(\rho_r^{2/3}T_r^{1/2})F(\rho_r,T_r)$, where the symbolic regression method was used to determine the functional form for $F(\rho_r,T_r)$. For this task, the dilute-gas limit and the initial density dependence terms were calculated for each experimental point (employing Eqs. (2) – (7)) and subtracted from the experimental viscosity to obtain the residual term. The density values employed were obtained by the equation of state of Qi *et al.*[21] The final equation obtained was

$$\Delta\eta(\rho,T)=\left(\rho_r^{2/3}T_r^{1/2}\right)\left\{c_0+c_1\rho_r+c_2T_r^2+c_3\rho_r^4+\frac{c_4(T_r+\rho_r)}{c_5T_r^2+T_r^2\rho_r^2}\right\}. \quad (8)$$

Coefficients c_i are given in Table 4.

3. Thermal Conductivity Methodology

In a very similar fashion to that described for the expression of viscosity in Section 2, the thermal conductivity λ is expressed as the sum of three independent contributions, as

$$\lambda(\rho,T)=\lambda_{\mathrm{o}}(T)+\Delta\lambda(\rho,T)+\Delta\lambda_{\mathrm{c}}(\rho,T), \quad (9)$$

where ρ is the density, T is the temperature, and the first term, $\lambda_o(T) = \lambda(0,T)$, is the contribution to the thermal conductivity in the dilute-gas limit, where only two-body molecular interactions occur. The final term, $\Delta\lambda_c(\rho,T)$, the critical enhancement, arises from the long-range density fluctuations that occur in a fluid near its critical point, which contribute to divergence of the thermal conductivity at the critical point. Finally, the term $\Delta\lambda(\rho,T)$, the residual property, represents the contribution of all other effects to the thermal conductivity of the fluid at elevated densities.

Table 5 summarizes, to the best of our knowledge, the experimental measurements[41, 42] of the thermal conductivity of R161 reported in the literature. There are only two sets of data. Wu *et al.*[41] recently measured the thermal conductivity of R161 in a transient hot-wire apparatus, with an estimated uncertainty of 1%. All measurements are in the liquid phase, and cover a wide range of temperature (234 K – 373 K) at pressures up to 20 MPa. Yao *et al.*[42] also measured the thermal conductivity of R161 in a transient hot-wire apparatus. Measurements were made in both the gas and liquid phases, with estimated uncertainties of 3% for the gas and 2% for the liquid. They also made some measurements very close to the critical point. For the primary data set, we included all points from Wu *et al.*[41] and most of the points from Yao *et al.*[42] We did not include as primary data any of the Yao *et al.*[42] data in the density range 200 kg m^3 < ρ < 600 kg m^3, as these points correspond to the near critical region. Yao *et al.*[42] report thermal conductivity data for R161 along the saturated liquid line and in the vapor phase at temperatures up to the critical temperature. The data in the critical region include about 23 gas points at temperatures from 373 K to 380.5 K; 13 points are at temperatures above the critical temperature of 375.25 K. The value of the critical temperature is from measurements by Beyerlein *et al.*[43] There are 9 “saturated liquid” data points in Yao *et al.*[42] at temperatures from 374.5 K to 375.2 K, with 3 points within 0.05 K of the critical temperature. The apparent critical enhancement in the data of Yao *et al.*[42] is much smaller than expected based on the critical point determined by Beyerlein *et al.*[43] Examination of the purities of the samples of R161 used in both studies reveals that the purity of the Yao *et al.*[42] sample was 99.95 mass %, while Beyerlein *et al.*[43] reported they studied a commercial sample and did not indicate its purity. The critical point reported by Beyerlein *et al.*[43] was used by Qi *et al.*[21] in the development of the equation of state used in the present work. Qi *et al.*[21] also reported density measurements made on a sample of R161 with a purity of 99.74 mass %. In addition, Qi *et al.*[21] show that vapor pressures reported by Beyerlein *et al.*[43] are higher by (2 to 4) % than other data sets measured on pure samples of R161. This discrepancy indicates that the purity of the sample of R161 measured by Beyerlein *et al.*[43] may have introduced error in their reported critical temperature, pressure, and density values. This may be the reason for the apparent discrepancy between the thermal conductivity data of Yao *et al.*[42] and theory incorporating the equation of state of Qi *et al.*[21] Since the data of Yao *et al.*[42] in the critical region are not consistent with the critical point in the equation of state of Qi *et al.*,[21] it was decided to omit these points from the primary data set. The final primary data set consisted of 238 points in the liquid phase, and 195 points in the gas phase.

Figures 3 and 4 show the range of the primary measurements outlined in Table 5, along with the saturation curve. The development of the correlation requires accurate values for the density, and as was done with the viscosity correlation, we use the recently published EOS of Qi *et al.*[21] to provide densities.

3.1. The thermal conductivity dilute-gas limit

In order to be able to extrapolate the temperature range of the measurements, a theoretically-based scheme was preferred in order to correlate the dilute-gas limit thermal conductivity, $\lambda_o(T)$, over a wide temperature range. The traditional kinetic approach for thermal conductivity results in an expression involving three generalized cross sections.[44, 45] However, it is possible to derive an equivalent kinetic theory expression for thermal conductivity by making use of the approach of Thijsse *et al.*[46] and Millat *et al.*,[47] where one considers expansion in terms of total energy, rather than separating translational from internal energy as is done traditionally. In this case, the dilute-gas limit thermal conductivity, $\lambda_o(T)$ (mW m^{-1} K^{-1}), of a polyatomic gas can be shown to be inversely proportional to a single generalized cross section,[44–47] $S(10E)$ (nm^2), as

$$\lambda_{\mathrm{o}}(T)=1000\frac{5k_{\mathrm{B}}^2(1+r^2)T}{2m\langle\nu\rangle_{\mathrm{o}}S(10E)}f_\lambda, \quad (10)$$

where k_B is the Boltzmann constant, T (K) is the absolute temperature, f_λ (−) is the dimensionless higher-order correction factor, m (kg) is the molecular mass of R161, and $\langle\nu\rangle_{\mathrm{o}}=4\sqrt{k_{\mathrm{B}}T/\pi m}$ (m/s) is the average relative thermal speed. The quantity r^2 is defined by $r^2=2C^{\mathrm{o}}_{\mathrm{int}}/5k_{\mathrm{B}}$, where $C^{\mathrm{o}}_{\mathrm{int}}$ is the contribution of both the rotational, $C^{\mathrm{o}}_{\mathrm{rot}}$, and the vibrational, $C^{\mathrm{o}}_{\mathrm{vib}}$, degrees of freedom to the isochoric ideal-gas heat capacity C^{o}_{ν}.

The recent classical trajectory calculations[48–50] confirm that, for most molecules studied, the higher-order thermal-conductivity correction factor is near unity. One can take advantage of this finding to define the effective generalized cross section S_λ (= $S(10E)/f_\lambda$) (nm^2), and rewrite Eq. (10) for the dilute-gas limit thermal conductivity of R161, $\lambda_o(T)$ (mW m^{-1} K^{-1}), as

$$\lambda_0(T)=0.0804686\frac{(C^{\mathrm{o}}_p/k_{\mathrm{B}})\sqrt{T}}{S_\lambda}. \quad (11)$$

The ideal-gas isobaric heat capacity per molecule, $C^{\mathrm{o}}_p(=C^{\mathrm{o}}_{\mathrm{int}}+2.5k_{\mathrm{B}})$ in (J/K), can be obtained from Qi *et al.*[21] as

$$\frac{C^o_p}{k_{\mathrm{B}}}=4+\sum_{k=1}^{4}\nu_k\left(\frac{u_k}{T}\right)^2\frac{\exp(u_kT)}{[\exp(u_kT)-1]^2}, \quad (12)$$

where the values of the coefficients ν_k and u_k are: ν_1 = 1.088 88, ν_2 = 1.808 42, ν_3 = 8.72 417, ν_4 = 5.677 15, u_1 = 329 K, u_2 = 742 K, u_3 = 1644 K, u_4 = 3922 K.

It has been previously noted,[47] and recently confirmed[45] for smaller molecules, that the cross section $S(10E)$ exhibits a nearly linear dependence on the inverse temperature. Hence, in order to develop the correlation, we have fitted the effective cross section S_λ (nm^2), obtained from the low-density data of Yao *et al.*[42] that was developed based on their experimental data over the temperature range 235 K to 375 K by means of Eq. (11), to a polynomial in inverse temperature, resulting in the following expression:

$$S_\lambda = -0.526931 + \frac{9.90063 \times 10^2}{T} - \frac{3.36966 \times 10^5}{T^2} + \frac{4.34209 \times 10^7}{T^3}. \quad (13)$$

Equations (11) – (13) form a consistent set of equations for the calculation of the dilute-gas limit thermal conductivity of R161.

The values of the dilute–gas limit thermal conductivity, $\lambda_0(T)$ in mW m^{-1} K^{-1}, obtained by the scheme of Eqs. (11) – (13), were fitted as a function of the reduced temperature $T_r = T / T_c$ for ease of use to the following equation:

$$\lambda_0(T) = \frac{7.96804 - 12.5874T_r - 26.3743T_r^2 + 16.9894T_r^3 + 127.545T_r^4 - 32.548T_r^5}{5.406 - 18.8331T_r + 24.868T_r^2 - 9.14139T_r^3 + T_r^4}. \quad (14)$$

Values calculated by Eq. (14) do not deviate from the values calculated by the scheme of Eqs. (11) – (13) by more than 0.003% over the temperature range from 235 K to 1000 K. Equation (14) is hence employed in the calculations that will follow.

3.2. The thermal conductivity residual term

The thermal conductivities of pure fluids exhibit an enhancement over a large range of densities and temperatures around the critical point and become infinite at the critical point. This behavior can be described by models that produce a smooth crossover from the singular behavior of the thermal conductivity asymptotically close to the critical point to the residual values far away from the critical point.[35, 51, 52] The density-dependent terms for thermal conductivity can be grouped according to Eq. (9) as $[\Delta\lambda(\rho,T) + \Delta\lambda_c(\rho,T)]$. To assess the critical enhancement theoretically, we need to evaluate, in addition to the dilute-gas thermal conductivity, the residual thermal-conductivity contribution. The procedure adopted during this analysis used ODRPACK (Ref.[53]) to fit all the primary data simultaneously to the residual thermal conductivity and the critical enhancement, while maintaining the values of the dilute-gas thermal-conductivity data already obtained. The density values employed were obtained by the equation of state of Qi *et al.*[21] The primary data were weighted in inverse proportion to the square of their uncertainty.

The residual thermal conductivity was represented with a polynomial in temperature and density:

$$\Delta\lambda(\rho,T)=\sum_{i=1}^{5}\left(B_{1,i}+B_{2,i}(T/T_{\mathrm{c}})\right)(\rho/\rho_{\mathrm{c}})^{i}. \quad (15)$$

Coefficients $B_{1,i}$ and $B_{2,i}$ are shown in Table 6.

3.3. The thermal conductivity critical enhancement term

The theoretically based crossover model proposed by Olchowy and Sengers[35, 51, 52] is complex and requires solution of a quartic system of equations in terms of complex variables. A simplified crossover model has also been proposed by Olchowy and Sengers.[54] The critical enhancement of the thermal conductivity from this simplified model is given by

$$\Delta\lambda_{\mathrm{c}}=\frac{\rho C_p R_{\mathrm{D}} k_{\mathrm{B}} T}{6\pi\overline{\eta}\xi}(\overline{\Omega}-\overline{\Omega}_0), \quad (16)$$

with

$$\overline{\Omega}=\frac{2}{\pi}\left[\left(\frac{C_p-C_\nu}{C_p}\right)\arctan(\overline{q}_{\mathrm{D}}\xi)+\frac{C_\nu}{C_p}\overline{q}_{\mathrm{D}}\xi\right] \quad (17)$$

and

$$\overline{\Omega}_0=\frac{2}{\pi}\left[1-\exp\left(-\frac{1}{(\overline{q}_{\mathrm{D}}\xi)^{-1}+(\overline{q}_{\mathrm{D}}\xi\rho_{\mathrm{c}}/\rho)^2/3}\right)\right]. \quad (18)$$

In Eqs. (16) – (18), $\bar{\eta}$ (Pa s) is the viscosity, and C_p and C_ν (J kg^{-1} K^{-1}) are the isobaric and isochoric specific heat obtained from the equation of state. The correlation length ξ (m) is given by

$$\xi=\xi_0\left(\frac{p_{\mathrm{c}}\rho}{\Gamma\rho_{\mathrm{c}}^2}\right)^{\nu/\gamma}\left[\left.\frac{\partial\rho(T,\rho)}{\partial p}\right|_T-\left(\frac{T_{\mathrm{ref}}}{T}\right)\left.\frac{\partial\rho(T_{\mathrm{ref}},\rho)}{\partial p}\right|_T\right]^{\nu/\gamma}. \quad (19)$$

As already mentioned, the coefficients $B_{1,i}$ and $B_{2,i}$ in Eq. (15) were fitted with ODRPACK (Ref.[53]) to the primary data for the thermal conductivity of R161. This crossover model requires the universal amplitude, R_{D} = 1.02 (−), and the universal critical exponents, ν = 0.63 and γ =1.239, and the system–dependent amplitudes Γ and ξ_0. For this work, we adopted the values Γ = 0.055 (−), ξ_0 = 0.183×10^{-9} m, using the universal representation of the critical enhancement of the thermal conductivity by Perkins *et al.*[55] When there are sufficient experimental data available in the critical region, the remaining parameter $\overline{q}_{\mathrm{D}}^{-1}(\mathrm{m})$ may be found by regression. However, as discussed earlier, the critical point in the equation

of state of Qi *et al.*[21] that is based on the data of Beyerlein *et al.*[43] may be in error, and in order to be consistent with the equation of state we cannot use the data of Yao *et al.*[42] in the critical region. We instead use the method of Perkins *et al.*[55] to estimate the effective cutoff wavelength $\bar{q}_{\mathrm{D}}^{-1}(\mathrm{m})$. The estimated value is 5.30×10^{-10} m. The viscosity required for Eq. (16) was calculated with the correlation developed earlier in this work. The reference temperature T_{ref}, far above the critical temperature where the critical enhancement is negligible, was calculated by $T_{\mathrm{ref}}=(3/2)T_{\mathrm{c}}$,[37] which for R161 is 562.88 K. Thus, the present critical enhancement calculation is consistent with the equation of state of Qi *et al.*[21] and should provide reasonable estimates of the thermal conductivity critical enhancement, although the uncertainty is larger in this area and further work may be necessary to determine the location of the critical point.

4. Evaluation of the Correlations

4.1 Viscosity

Figures 5 and 6 show the percentage deviations of the viscosity at low density $\Delta\eta_0 = \eta_0 + \eta_1\rho$, (calculated with Eq. (2) – (7) and the parameters in Tables 2 and 3) with the experimental viscosity values of Lv *et al.*,[28] (for pressures below 0.5 MPa) as a function of temperature and density. Although Eq. (7) was originally developed for propane, as in its recent application,[15, 16, 19, 20] the agreement is excellent. Thus, we estimate the uncertainty of the correlation for the low-density gas viscosity at temperatures from 290 K to 370 K to be 2%, at a 95% confidence level. Therefore, Eqs. (2) – (7) can be employed for the calculation of the dilute-gas limit viscosity, $\eta_0(T)$ and the initial density dependence term, $\eta_1(T)$.

Table 7 summarizes comparisons of the primary data with the correlation. We have defined the percent deviation as PCTDEV = $100*(\eta_{\mathrm{exp}}-\eta_{\mathrm{fit}})/\eta_{\mathrm{fit}}$, where η_{exp} is the experimental value of the viscosity and η_{fit} is the value calculated from the correlation. Thus, the average absolute percent deviation (AAD) is found with the expression AAD = $(\Sigma|\mathrm{PCTDEV}|)/n$, where the summation is over all n points, the bias percent is found with the expression BIAS = $(\Sigma\mathrm{PCTDEV})/n$. The average absolute percent deviation of the fit is 0.95%, and its bias is 0.52%. We estimate the uncertainty at a 95% confidence level to be 3%, except for the very-near critical region where the deviations are larger. As mentioned previously, we estimate the expanded uncertainty of the correlation at a 95% confidence level for the low-density gas at temperatures from 290 K to 370 K and pressures up to 0.5 MPa to be 2%.

Figure 7 shows the percentage deviations of all primary viscosity data from the values calculated by Eqs. (1) – (8), as a function of temperature, while Figs. 8 and 9 show the same deviations but as a function of the pressure and the density. All measurements are within 3% except 12 measurements of Fan *et al.*[29] at the lower and higher temperatures, that extend from –5% to 8%.

4.2 Thermal Conductivity

Figure 10 presents the percentage deviations of the low-density (densities below 15 kg m^{-3}, corresponding to pressures below 0.9 MPa) experimental data from the values calculated by Eq. (14). The selected data are represented within the uncertainty of the data, 3%. No

obvious systematic trends are observed. Therefore, based on the aforementioned discussion, Eqs. (11) – (13) or Eq. (14) represent the dilute-gas limit thermal conductivity to within 3% at the 95% confidence level.

Table 8 summarizes comparisons of the primary data with the correlation. We have defined the percentage deviation as PCTDEV = $100*(\lambda_{exp}-\lambda_{fit})/\lambda_{fit}$, where λ_{exp} is the experimental value of the thermal conductivity and λ_{fit} is the value calculated from the correlation. The AAD and BIAS are as defined in Section 4.1. We estimate the uncertainty (at the 95% confidence level) for the thermal conductivity in the liquid phase from 234 K to 374 K at pressures up to 20 MPa to be 3%. For the gas phase, the estimated uncertainty is 3% at densities below 15 kg m^{-3} and 4% at higher densities. Uncertainties in the critical region are much larger, since the thermal conductivity approaches infinity at the critical point and is very sensitive to small changes in density. In addition, as mentioned earlier, the location of the critical point may be in error.

Figure 11 shows the percentage deviations of all primary thermal–conductivity data from the values calculated by Eqs. (9), (14) – (19), as a function of density. Points that were not included in the primary set due to their closeness to the critical point, are not shown in the figure. As noted by Yao et al.,[42] their experimental data did not show an enhancement in the critical region, and this results in some points near the critical point being as much as ~70% lower than what is predicted by the present correlation (with the critical point as given by the equation of state of Qi et al.[21]) We recommend that future measurements be made to determine the location of the critical point. Figures 12 and 13 show the same deviations of the primary data with the correlation, but as a function of temperature and pressure, respectively.

5. Recommended Values and Computer-Program Verification

5.1 Recommended Values

In Table 9, viscosity values are given along the saturated liquid line, calculated from the present proposed correlation between 250 and 375 K, while in Table 10 viscosity values are given for temperatures between 250 and 350 K and at 10 and 20 MPa. In both tables, values for the thermal conductivity calculated in Section 3 are also included. Saturation pressure and saturation density values for selected temperatures, as well as the density values for the selected temperature and pressure, are obtained from the equation of state of Qi *et al.*[21]

Fig. 14 shows a plot of the viscosity of R161 as a function of the temperature for different pressures. The plot demonstrates the smooth extrapolation behavior at temperatures up to 600 K and pressures up to 50 MPa.

Finally, Figs. 15 and 16 show plots of the thermal conductivity of R161 as a function of the temperature for different pressures, and as a function of the density for different temperatures. The correlation behaves in a physically reasonable manner for extrapolations outside of the range of experimental data.

5.2 Computer-Program Verification

For checking computer implementations of the correlation, we provide Table 11. The points are calculated with the tabulated temperatures and densities.

6. Conclusions

New wide-ranging correlations for the viscosity and thermal conductivity of R161 were developed based on critically evaluated experimental data. The correlations are expressed in terms of temperature and density and are designed to be used with the equation of state of Qi *et al.*[21] that is valid from 130 K to 450 K, at pressures up to 100 MPa. The estimated uncertainty at a 95% confidence level is 2% for the viscosity of low-density gas (pressures below 0.5 MPa), and 3% for the viscosity of the liquid over the temperature range from 243 K to 363 K at pressures up to 30 MPa. The estimated uncertainty is 3% for the thermal conductivity of the low-density gas, and 3% for the liquid over the temperature range from 234 K to 374 K at pressures up to 20 MPa. Both correlations may be used over the full range of the equation of state but the uncertainties will be larger, especially in the critical region.

References

1. Assael MJ, Assael JAM, Huber ML, Perkins RA, Takata Y. J. Phys. Chem. Ref. Data. 2011; 40:033101.
2. Huber ML, Perkins RA, Friend DG, Sengers JV, Assael MJ, Metaxa IN, Miyagawa K, Hellmann R, Vogel E. J. Phys. Chem. Ref. Data. 2012; 41:033102.
3. Assael MJ, Koini IA, Antoniadis KD, Huber ML, Abdulagatov IM, Perkins RA. J. Phys. Chem. Ref. Data. 2012; 41:023104.
4. Huber ML, Sykioti EA, Assael MJ, Perkins RA. J. Phys. Chem. Ref. Data. 2016; 45:013102. [PubMed: 27064300]
5. Assael MJ, Mylona SK, Huber ML, Perkins RA. J. Phys. Chem. Ref. Data. 2012; 41:023101.
6. Assael MJ, Michailidou EK, Huber ML, Perkins RA. J. Phys. Chem. Ref. Data. 2012; 41:043102.
7. Assael MJ, Mylona SK, Huber ML, Perkins RA. J. Phys. Chem. Ref. Data. 2013; 42:013106.
8. Koutian A, Assael MJ, Huber ML, Perkins RA. J. Phys. Chem. Ref. Data. 2017; 46:013102. [PubMed: 28584386]
9. Assael MJ, Bogdanou I, Mylona SK, Huber ML, Perkins RA, Vesovic V. J. Phys. Chem. Ref. Data. 2013; 42:023101.
10. Sykioti EA, Assael MJ, Huber ML, Perkins RA. J. Phys. Chem. Ref. Data. 2013; 42:043101.
11. Assael MJ, Sykioti EA, Huber ML, Perkins RA. J. Phys. Chem. Ref. Data. 2013; 42:023102.
12. Assael MJ, Koutian A, Huber ML, Perkins RA. J. Phys. Chem. Ref. Data. 2016; 45:033104. [PubMed: 27818536]
13. Mylona SK, Antoniadis KD, Assael MJ, Huber ML, Perkins RA. J. Phys. Chem. Ref. Data. 2014; 43:043104.
14. Huber ML, Perkins RA, Laesecke A, Friend DG, Sengers JV, Assael MJ, Metaxa IN, Vogel E, Mares R, Miyagawa K. J. Phys. Chem. Ref. Data. 2009; 38:101.
15. Michailidou EK, Assael MJ, Huber ML, Perkins RA. J. Phys. Chem. Ref. Data. 2013; 42:033104.
16. Michailidou EK, Assael MJ, Huber ML, Abdulagatov I, Perkins RA. J. Phys. Chem. Ref. Data. 2014; 43:023103.
17. Avgeri S, Assael MJ, Huber ML, Perkins RA. J. Phys. Chem. Ref. Data. 2014; 43:033103.
18. Avgeri S, Assael MJ, Huber M, Perkins RA. J. Phys. Chem. Ref. Data. 2015; 44:033101.
19. Perkins RA, Huber ML, Assael MJ. J. Chem. Eng. Data. 2016; 61:3286.
20. Huber ML, Assael MJ. Int. J. Refrig. 2016; 71:45.

21. Qi H, Fang D, Gao K, Meng X, Wu J. Int. J. Thermophys. 2016; 37:55.
22. Assael MJ, Ramires MLV, Nieto de Castro CA, Wakeham WA. J. Phys. Chem. Ref. Data. 1990; 19:113.
23. Friend DG, Rainwater JC. Chem. Phys. Lett. 1984; 107:590.
24. Rainwater JC, Friend DG. Phys. Rev. A. 1987; 36:4062.
25. Bich, E., Vogel, E. Chap. 5.2, in Transport Properties of Fluids. Their Correlation, Prediction and Estimation. Cambridge University Press; Cambridge: 1996.
26. Bi S, Cui J, Meng X, Wu J. Fluid Phase Equilib. 2015; 405:25.
27. Meng X, Gu X, Wu J, Bi S. Int. J. Thermophys. 2015; 36:2497.
28. Lv S, Zhao X, Yao C, Wang W, Guo Z. Fluid Phase Equilib. 2014; 384:100.
29. Fan J, Zhao X, Guo Z, Liu Z. Int. J. Thermophys. 2012; 33:2243.
30. Vogel E, Küchenmeister C, Bich E, Laesecke A. J. Phys. Chem. Ref. Data. 1998; 27:947.
31. Maitland, GC., Rigby, M., Smith, EB., Wakeham, WA. Intermolecular Forces: Their Origin and Determination. Clarendon; Oxford: 1987.
32. Chapman, S., Cowling, TG. The Mathematical Theory of Non-Uniform Gases. Cambridge University Press; London: 1970.
33. Vogel E, Bich E, Nimz R. Physica A. 1986; 139:188.
34. Bhattacharjee JK, Ferrell RA, Basu RS, Sengers JV. Phys. Rev. A. 1981; 24:1469.
35. Olchowy GA, Sengers JV. Phys. Rev. Lett. 1988; 61:15. [PubMed: 10038682]
36. Luettmer-Strathmann J, Sengers JV, Olchowy GA. J. Chem. Phys. 1995; 103:7482.
37. Vesovic V, Wakeham WA, Olchowy GA, Sengers JV, Watson JTR, Millat J. J. Phys. Chem. Ref. Data. 1990; 19:763.
38. Hendl S, Millat J, Vogel E, Vesovic V, Wakeham WA, Luettmer-Strathmann J, Sengers JV, Assael MJ. Int. J. Thermophys. 1994; 15:1.
39. EUREQA Formulize v.098.1. Nutonian Inc.; Cambridge MA, USA:
40. Assael MJ, Dymond JH, Papadaki M, Patterson PM. Int. J. Thermophys. 1992; 13:269.
41. Wu J. Private Communication. 2016
42. Yao C, Zhao X, Lv S, Guo Z. Fluid Phase Equilib. 2014; 375:228.
43. Beyerlein AL, DesMarteau DD, Kul I, Zhao G. Fluid Phase Equilib. 1998; 150–151:287.
44. Hellmann R, Bich E, Vogel E, Vesovic V. J. Chem. Eng. Data. 2012; 57:1312.
45. McCourt, FRW., Beenakker, JJM., Köhler, WE., Kučšer, I. Nonequilibrium Phenomena in Polyatomic Gases. Clarendon Press; Oxford: 1990.
46. Thijsse BJ, Thooft GW, Coombe DA, Knaap HFP, Beenakker JJM. Physica A. 1979; 98:307.
47. Millat J, Vesovic V, Wakeham WA. Physica A. 1988; 148:153.
48. Bock S, Bich E, Vogel E, Dickinson AS, Vesovic V. J. Chem. Phys. 2004; 120:7987. [PubMed: 15267716]
49. Hellmann R, Bich E, Vogel E, Dickinson AS, Vesovic V. J. Chem. Phys. 2009; 130:124309. [PubMed: 19334832]
50. Hellmann R, Bich E, Vogel E, Vesovic V. Phys. Chem. Chem. Phys. 2011; 13:13749. [PubMed: 21720616]
51. Mostert R, van den Berg HR, van der Gulik PS, Sengers JV. J. Chem. Phys. 1990; 92:5454.
52. Perkins RA, Roder HM, Friend DG, Nieto de Castro CA. Physica A. 1991; 173:332.
53. Boggs, PT., Byrd, RH., Rogers, JE., Schnabel, RB. ODRPACK, Software for Orthogonal Distance Regression, NISTIR 4834, v2.013. National Institute of Standards and Technology; Gaithersburg, MD: 1992.
54. Olchowy GA, Sengers JV. Int. J. Thermophys. 1989; 10:417.
55. Perkins RA, Sengers JV, Abdulagatov IM, Huber ML. Int. J. Thermophys. 2013; 34:191.

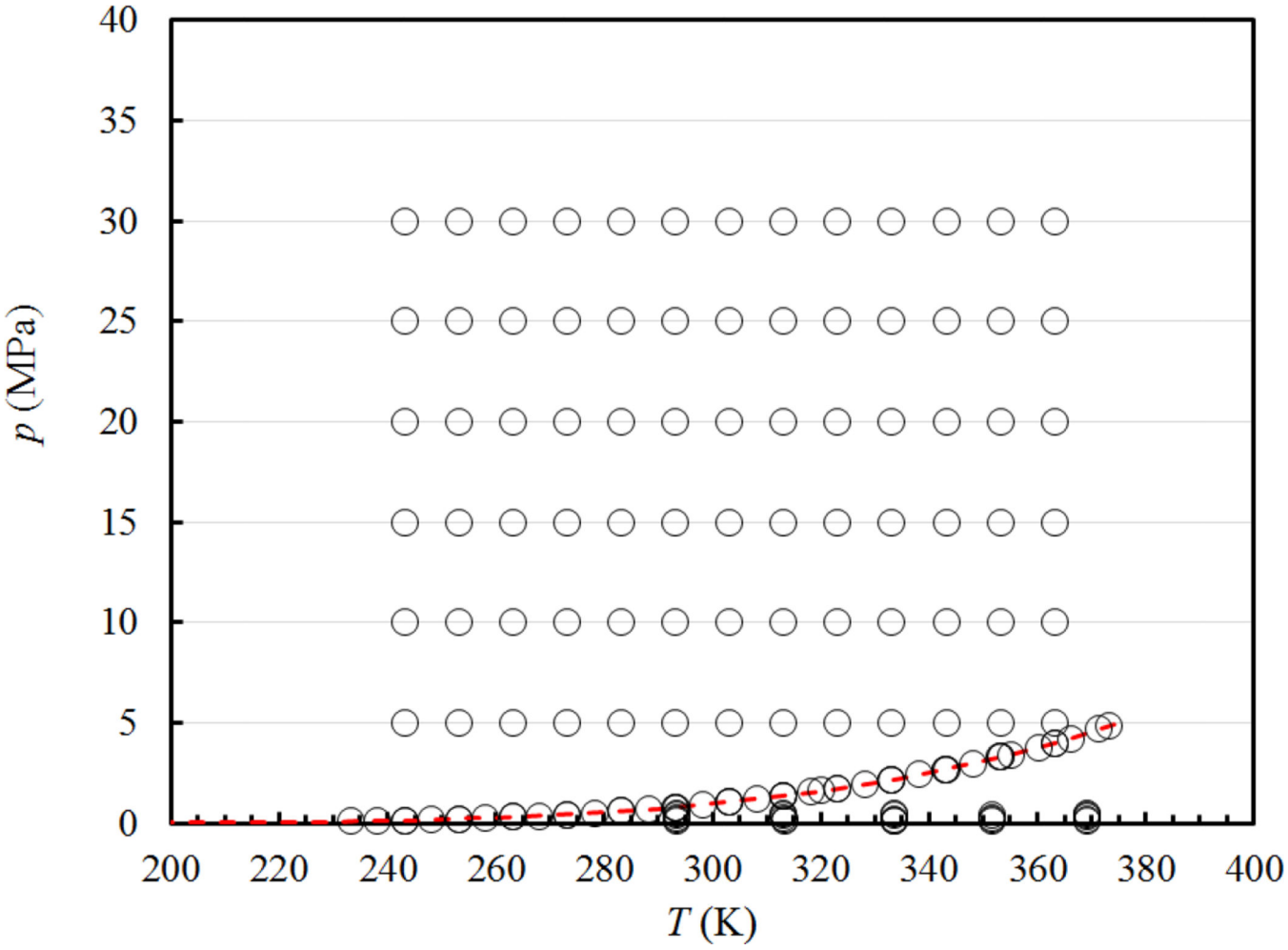

FIGURE 1.
Temperature-pressure ranges of the primary experimental viscosity data for R161.

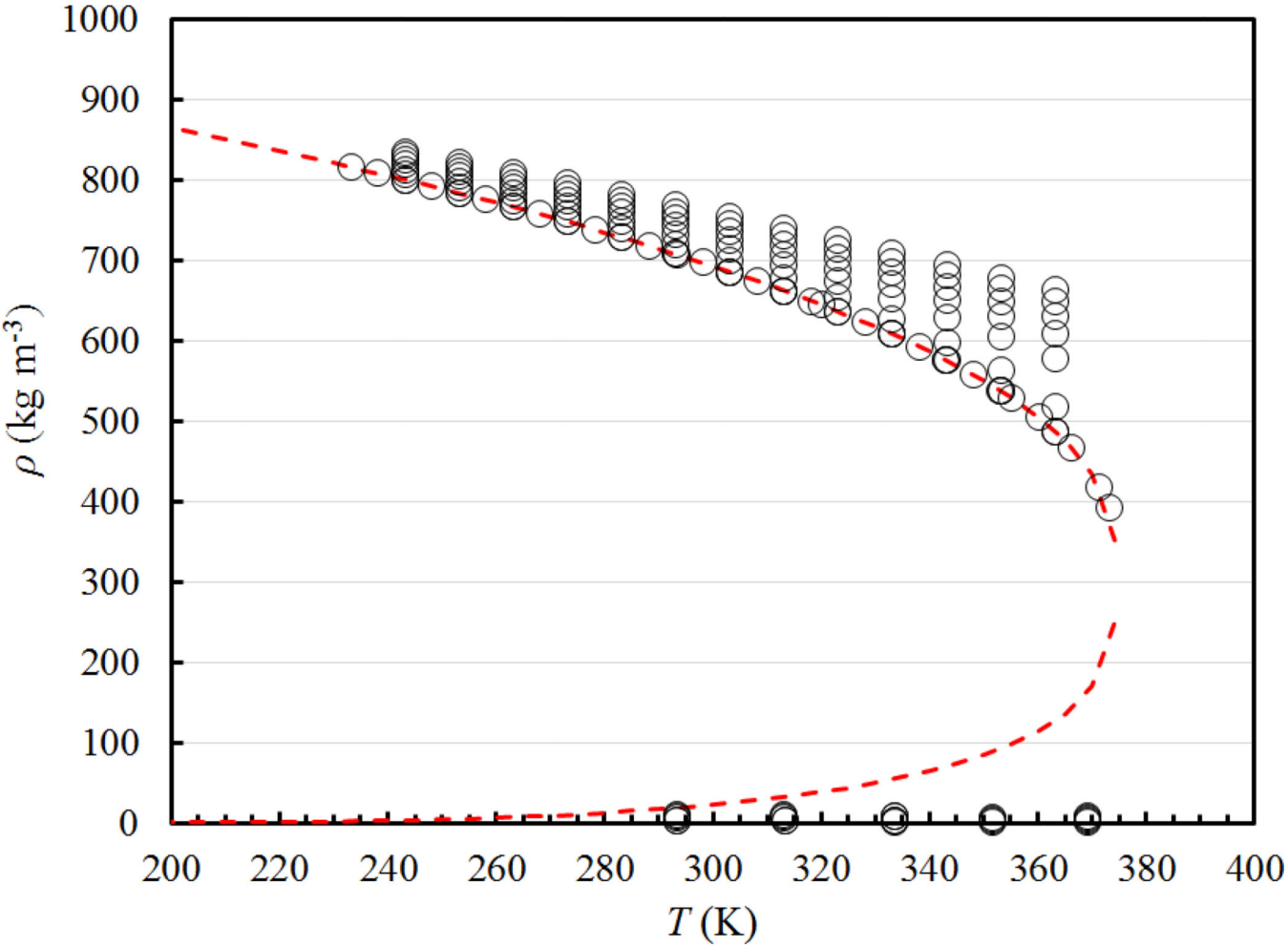

FIGURE 2.
Temperature-density ranges of the primary experimental viscosity data for R161.

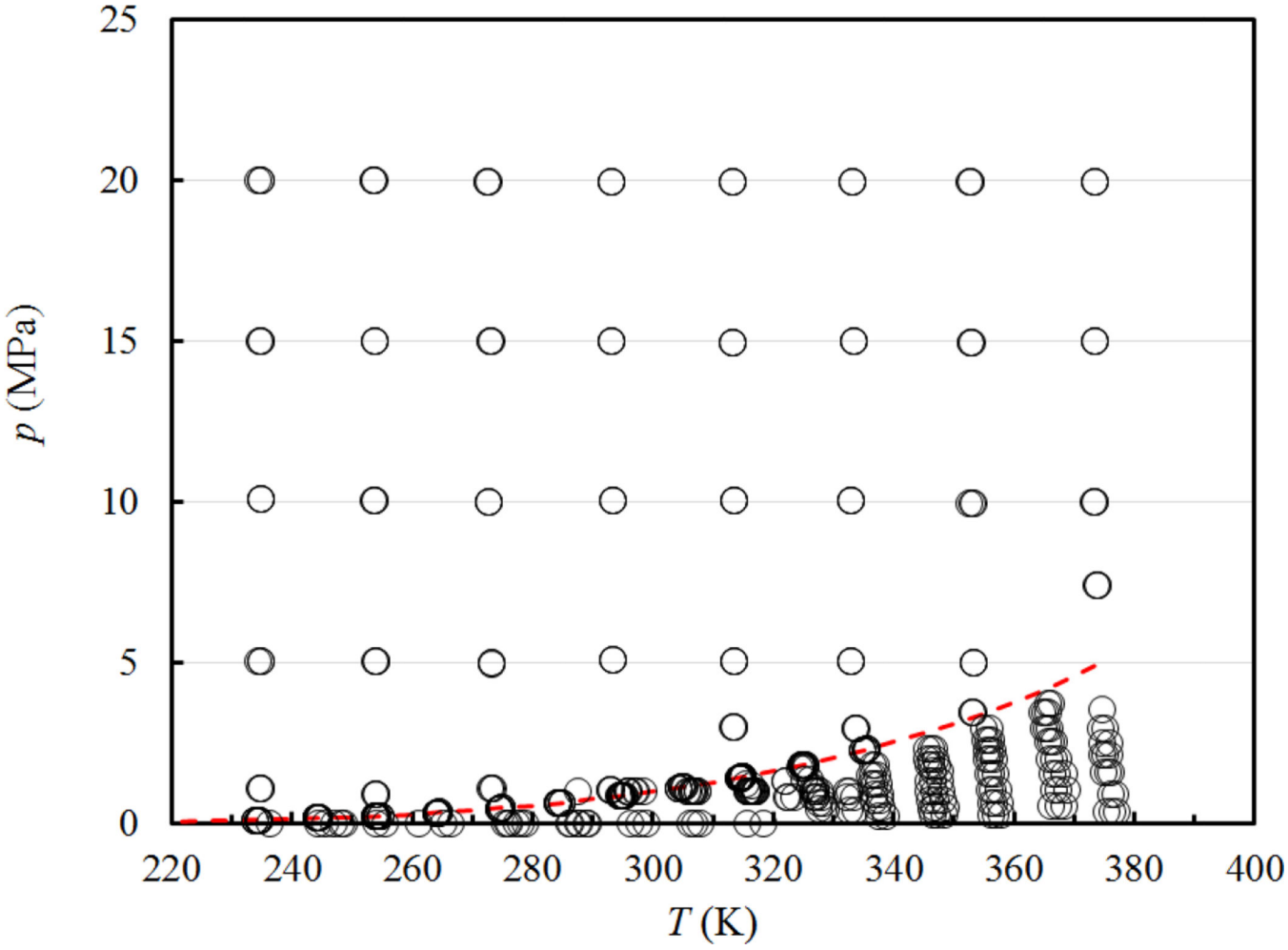

FIGURE 3.
Temperature–pressure range of the primary experimental thermal conductivity data for R161.

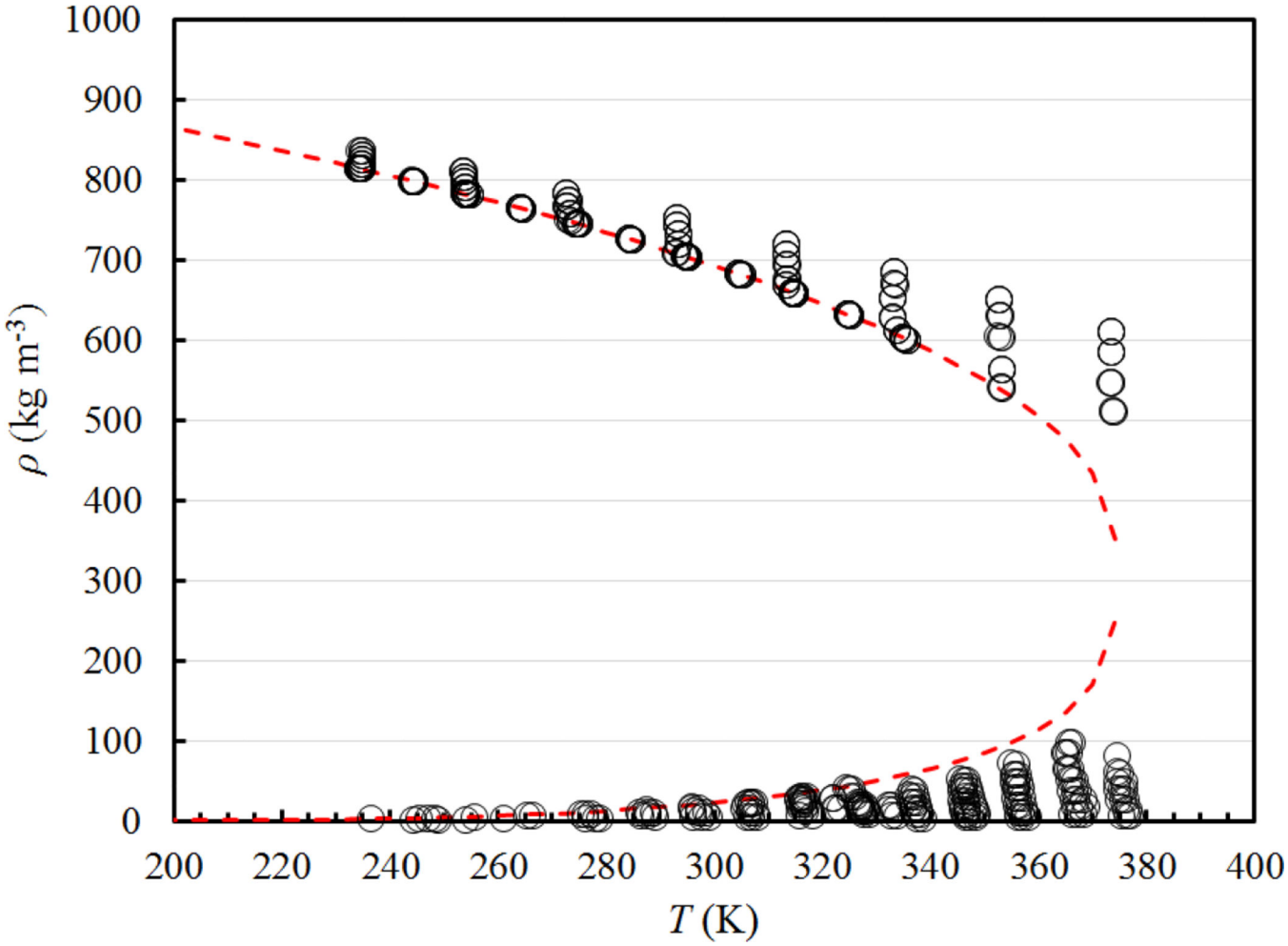

FIGURE 4.

Temperature–density range of the primary experimental thermal conductivity data for R161. (− −) saturation curve.

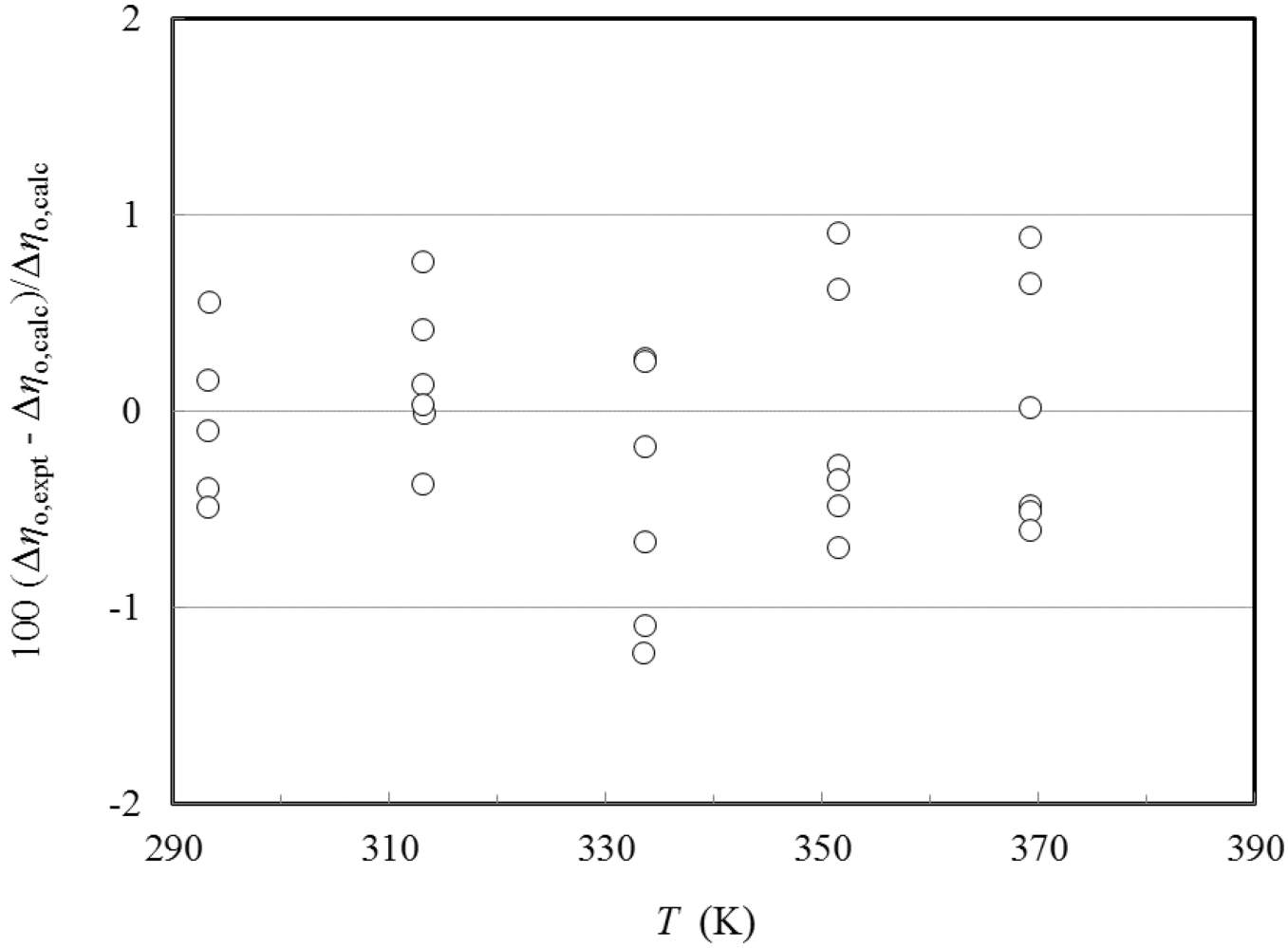

FIGURE 5.

Percentage deviations of the experimental low-density viscosity, $\Delta\eta_0 = \eta_0 + \eta_1 \rho$, of R161, from those calculated with Eqs. (2) – (7) with the parameters in Tables 2 and 3 as a function of temperature. (o) Lv *et al.*[28]

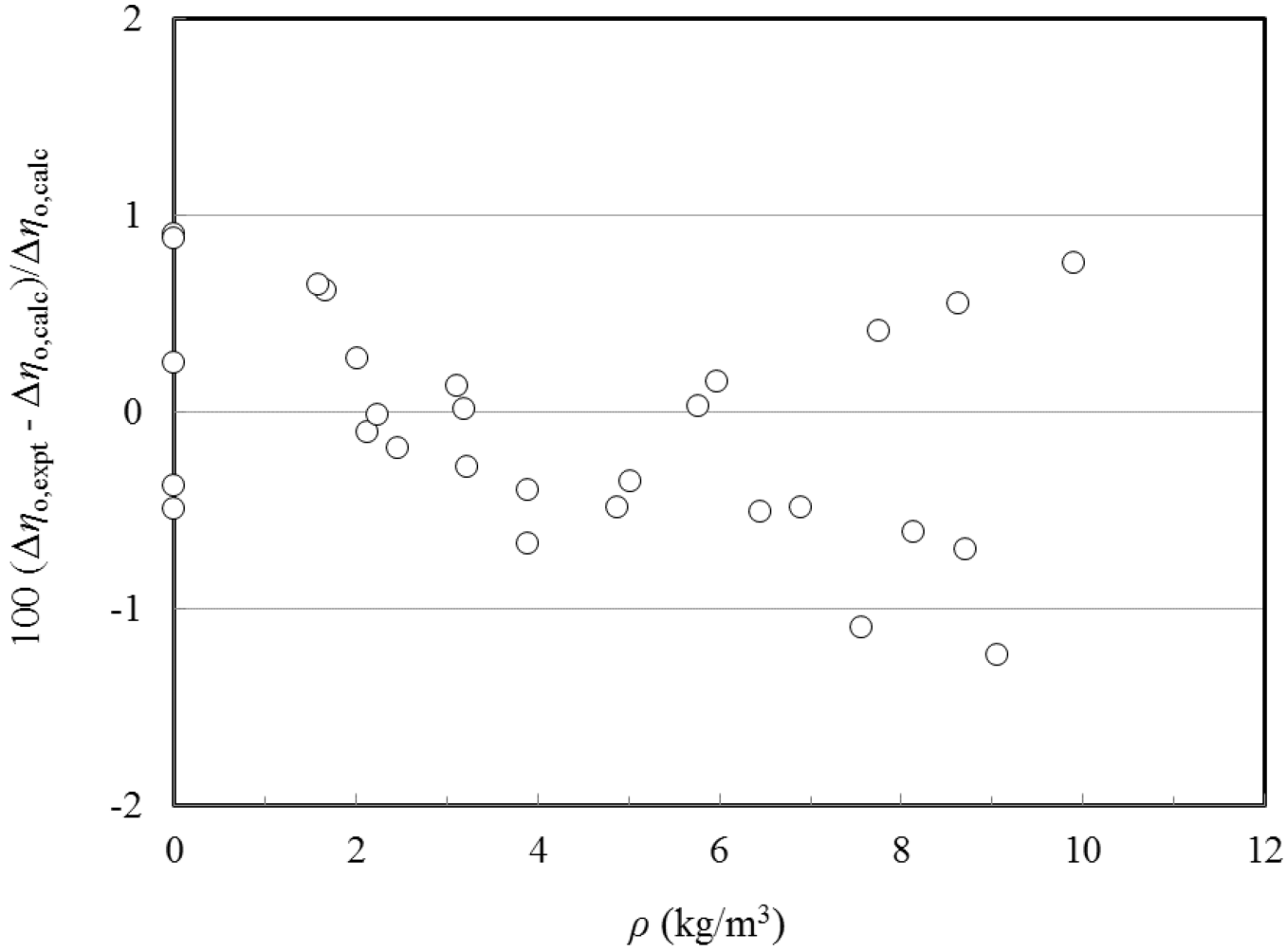

FIGURE 6.

Percentage deviations of the experimental low-density viscosity, $\Delta\eta = \eta_0 + \eta_1 \rho$, of R161, from those calculated with Eqs. (2) – (7) with the parameters in Tables 2 and 3, as a function of density. (o) Lv *et al.*[28]

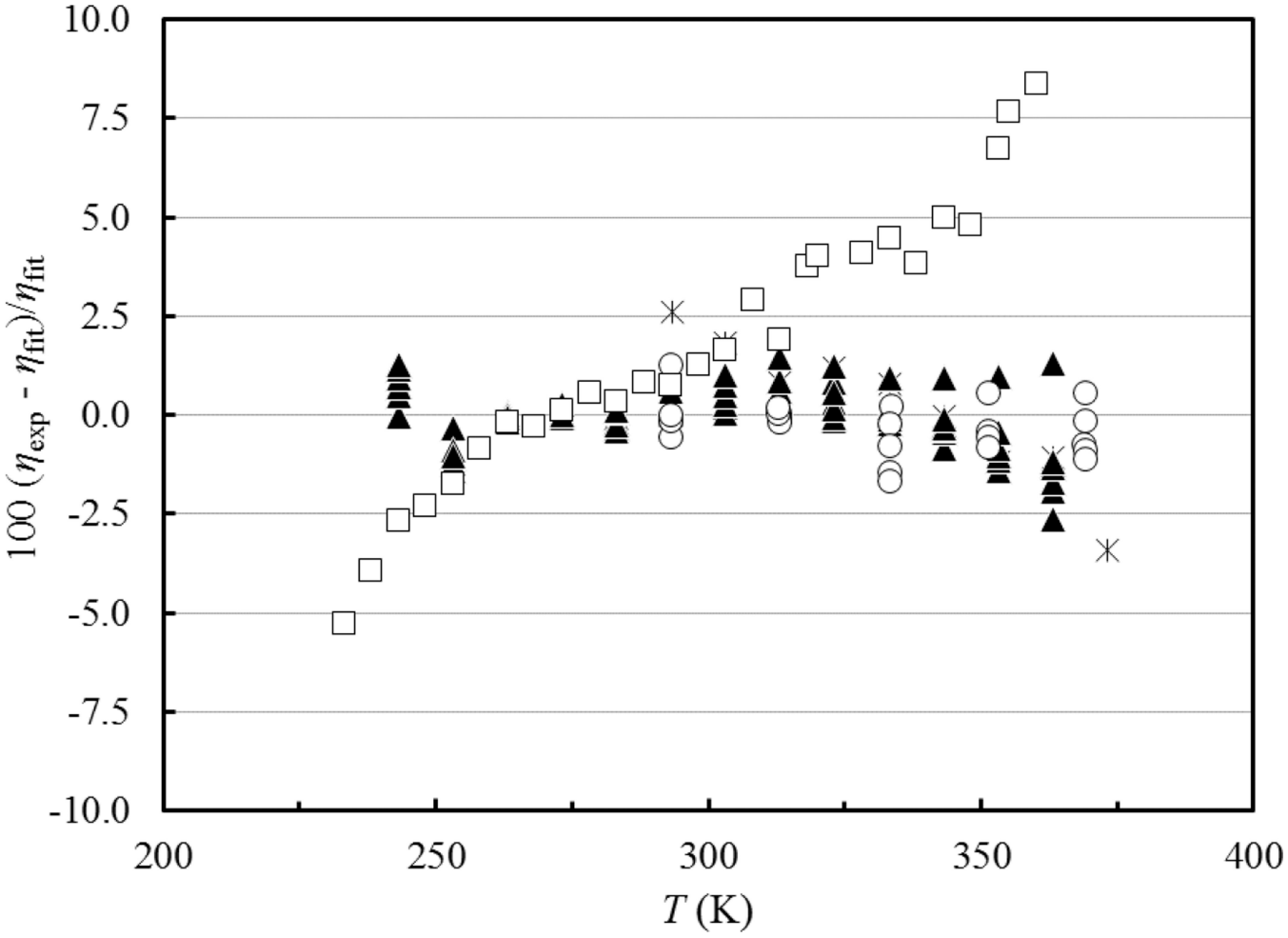

FIGURE 7.

Percentage deviations of primary viscosity experimental data of R161 from the values calculated by the present model as a function of temperature. Bi *et al.*[26](∗), Meng *et al.*[27](▲), Lv *et al.*[28](○), Fan *et al.*[29](□).

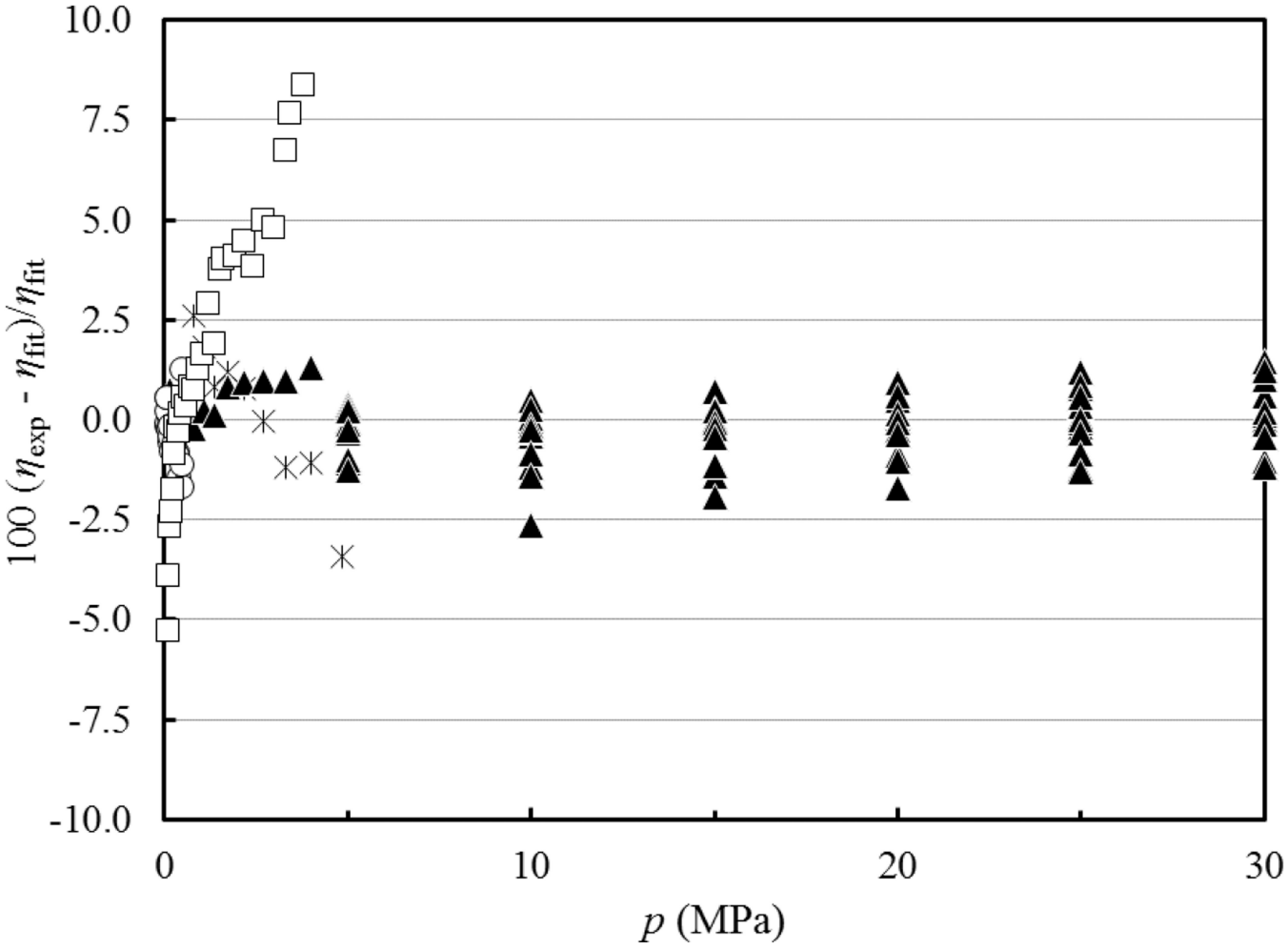

FIGURE 8.

Percentage deviations of primary viscosity experimental data of R161 from the values calculated by the present model as a function of pressure. Bi *et al.*[26](∗), Meng *et al.*[27](▲), Lv *et al.*[28](○), Fan *et al.*[29](□).

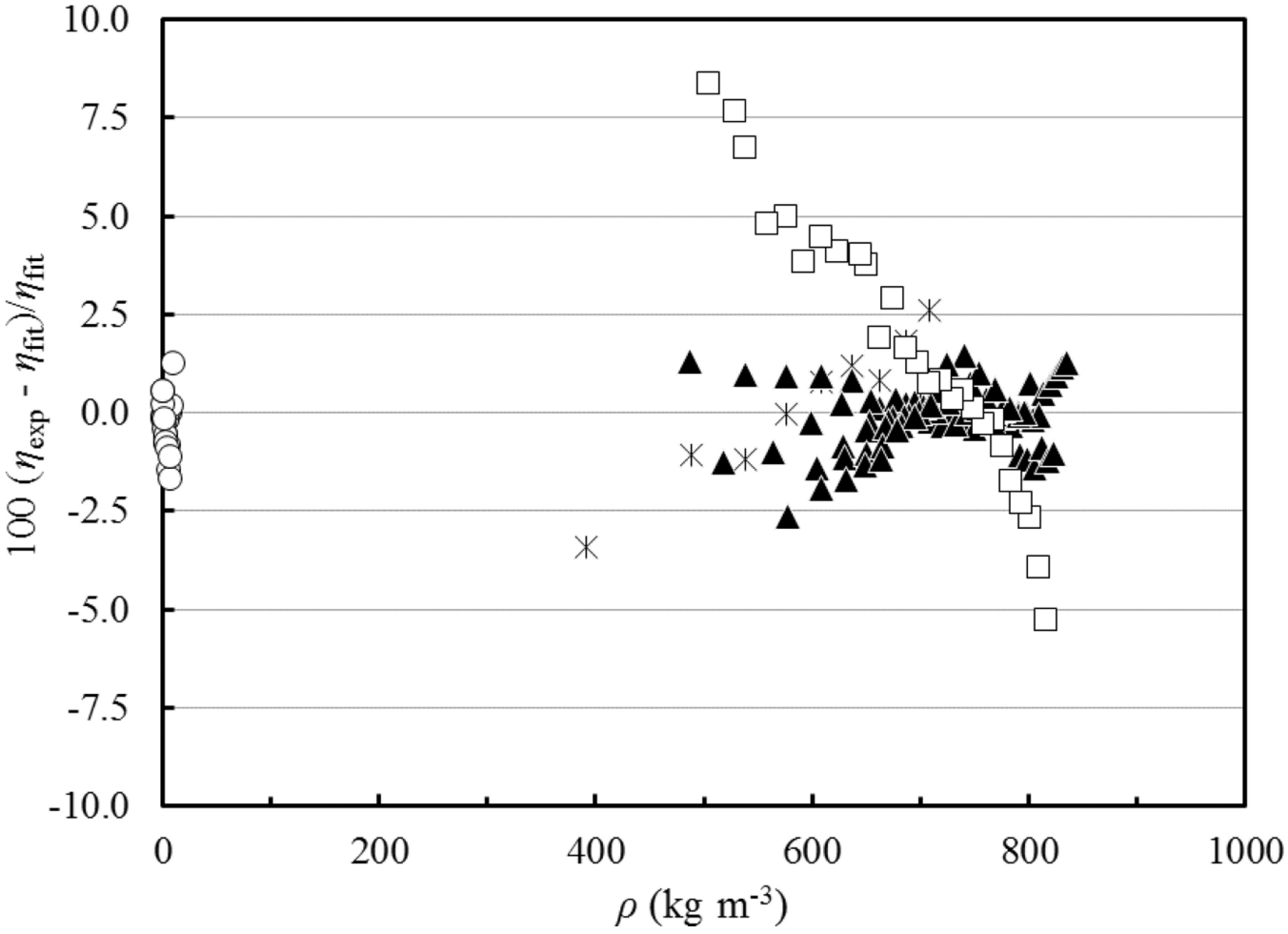

FIGURE 9.

Percentage deviations of primary viscosity experimental data of R161 from the values calculated by the present model as a function of density. Bi *et al.*[26](∗), Meng *et al.*[27](▲), Lv *et al.*[28](○), Fan *et al.*[29](□)

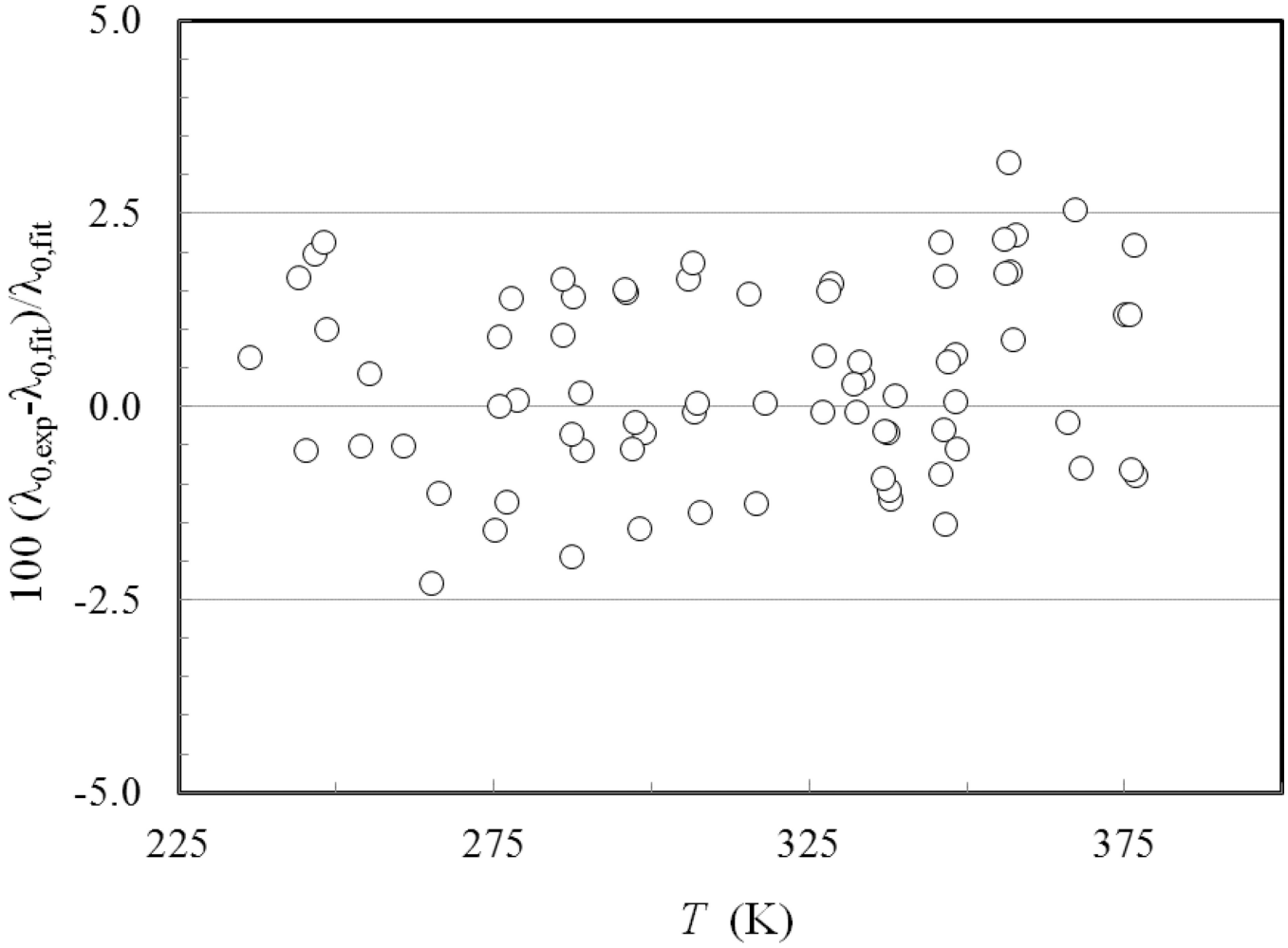

FIGURE 10.

Percentage deviations of the dilute-gas limit thermal-conductivity measurements of R161 from Eq. (14) as a function of temperature, experimental data of Yao *et al.*[42] (○).

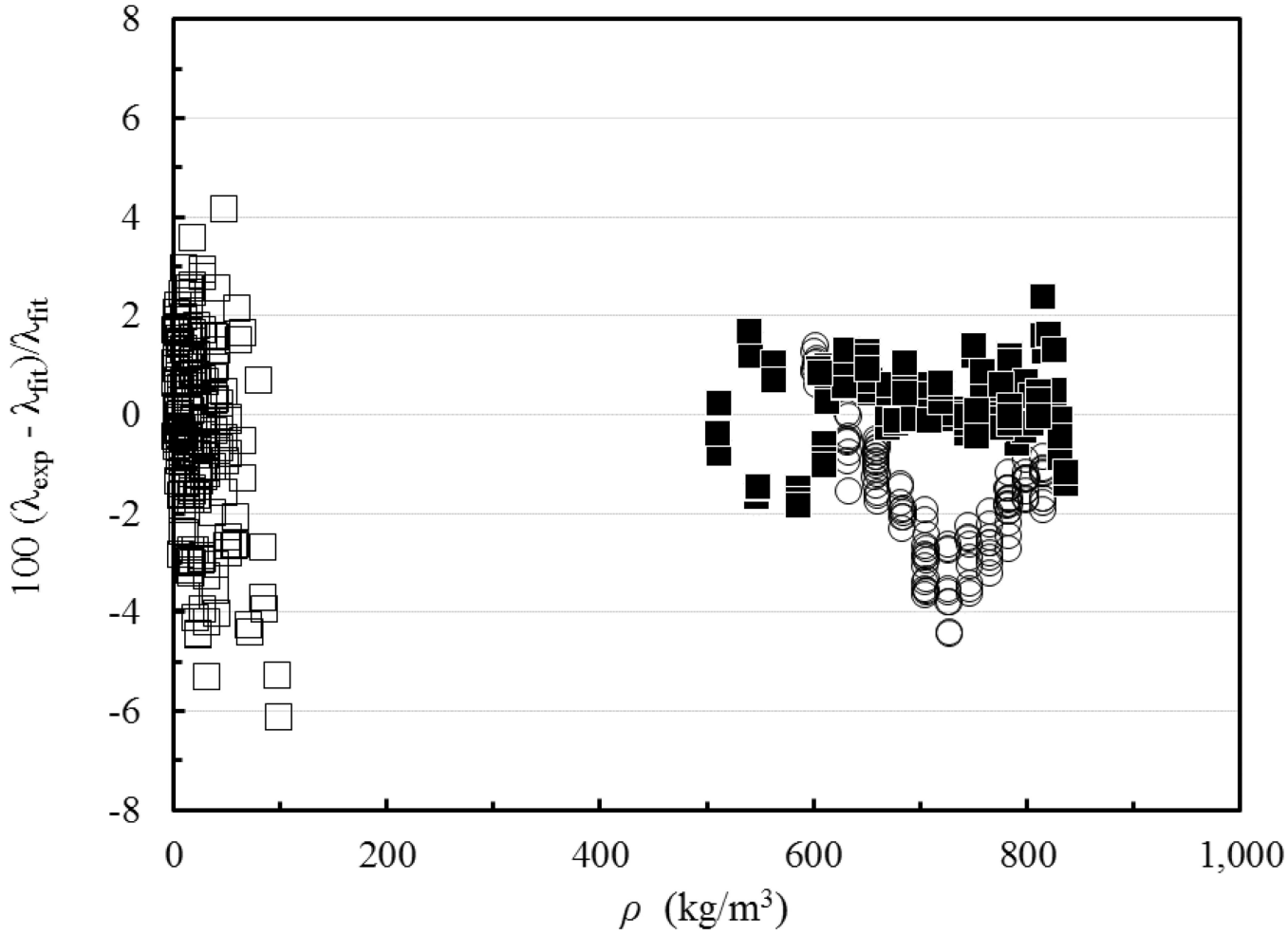

FIGURE 11.

Percentage deviations of primary thermal conductivity experimental data of R161 from the values calculated by the present model, Eqs. (9), (14) – (19), as a function of density. Wu *et al.*[41] (■), Yao *et al.*[42] (vapor) (□), Yao *et al.*[42] (liquid) (○).

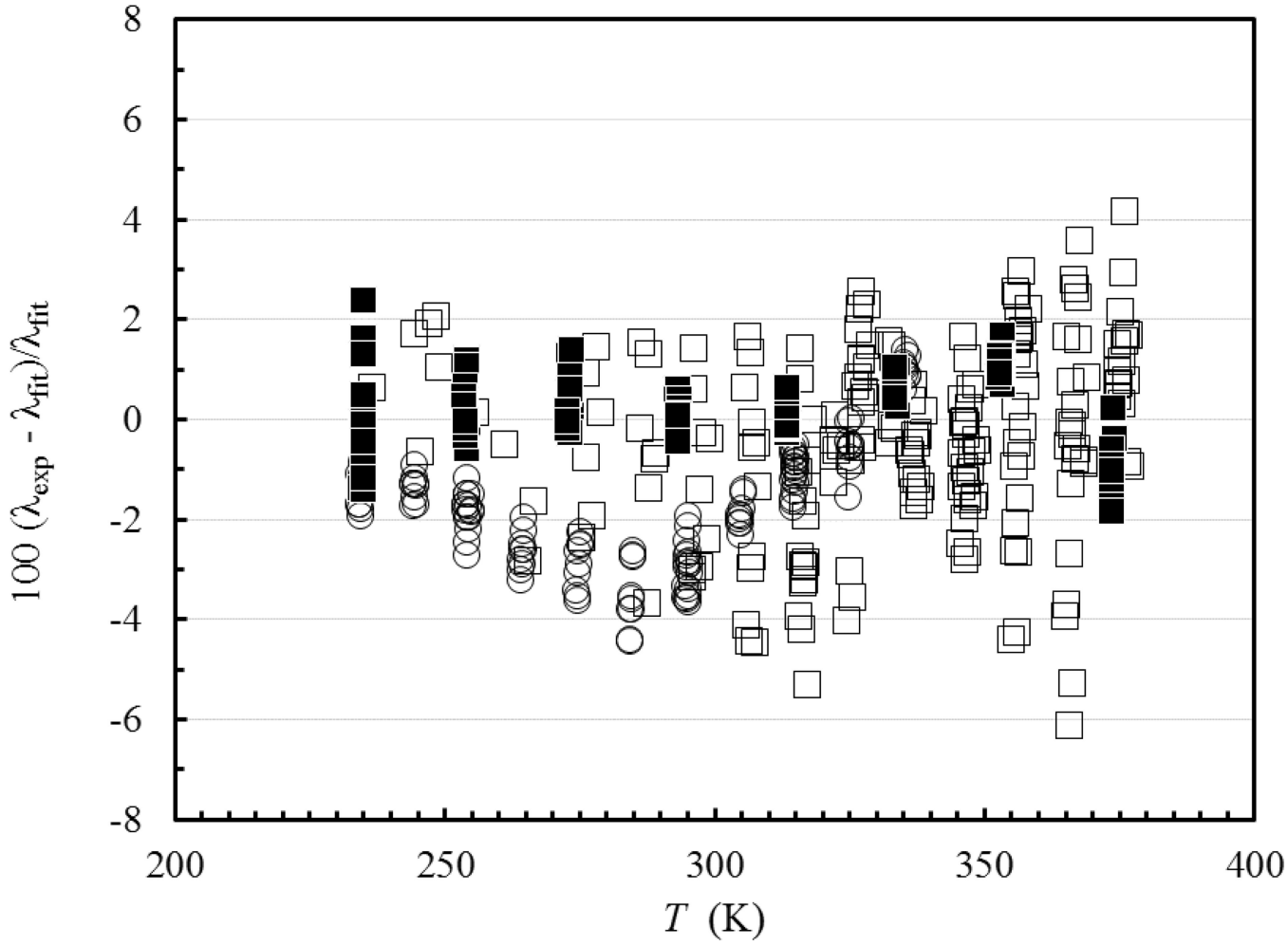

FIGURE 12.

Percentage deviations of primary thermal conductivity experimental data of R161 from the values calculated by the present model, Eqs. (9), (14) – (19), as a function of temperature. Wu *et al.*[41] (■), Yao *et al.*[42] (vapor) (□), Yao *et al.*[42] (liquid) (○).

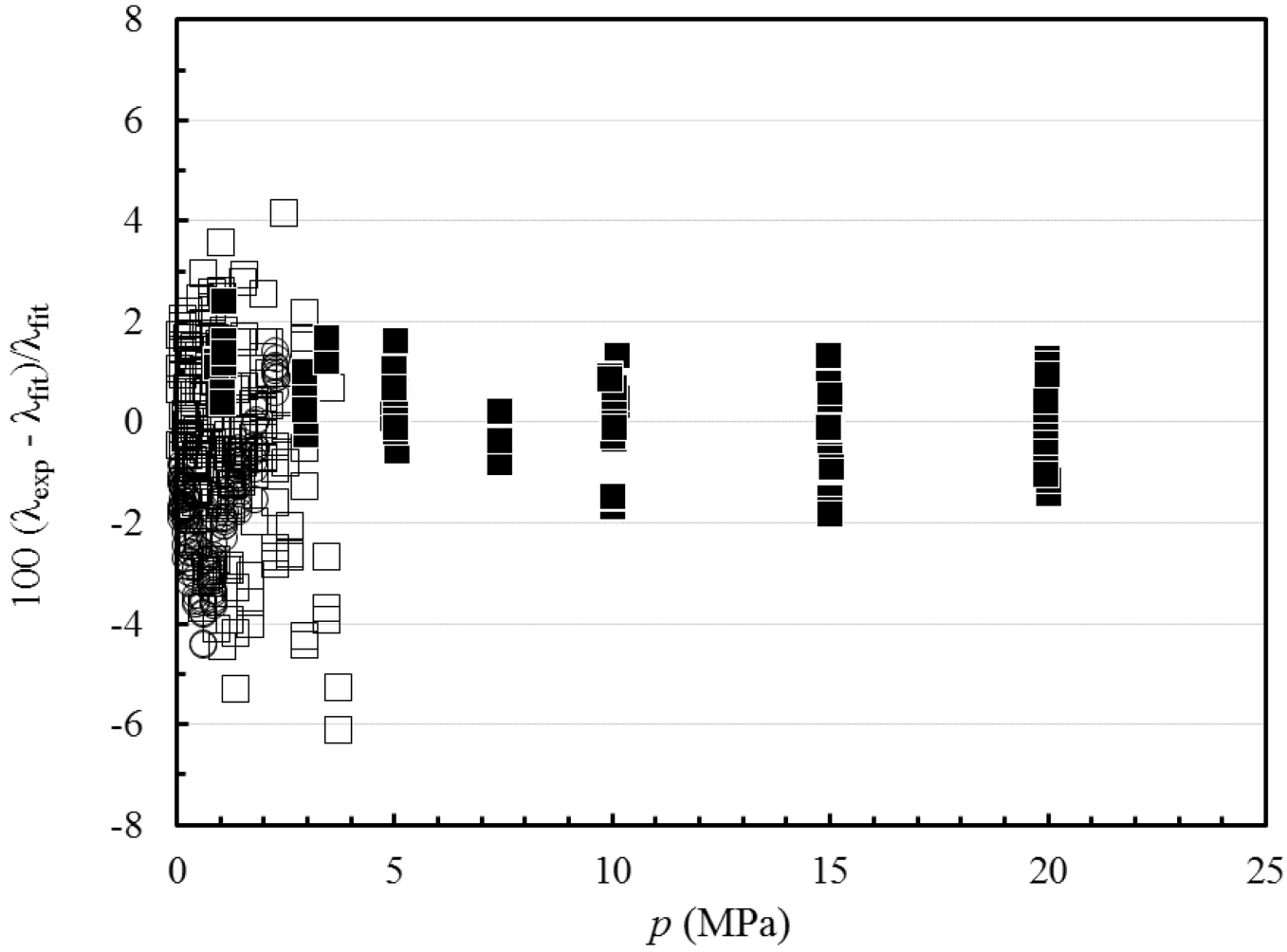

FIGURE 13.

Percentage deviations of primary thermal conductivity experimental data of R161 from the values calculated by the present model, Eqs. (9), (14) – (19), as a function of pressure. Wu *et al.*[41] (■), Yao *et al.*[42] (vapor) (□), Yao *et al.*[42] (liquid) (○).

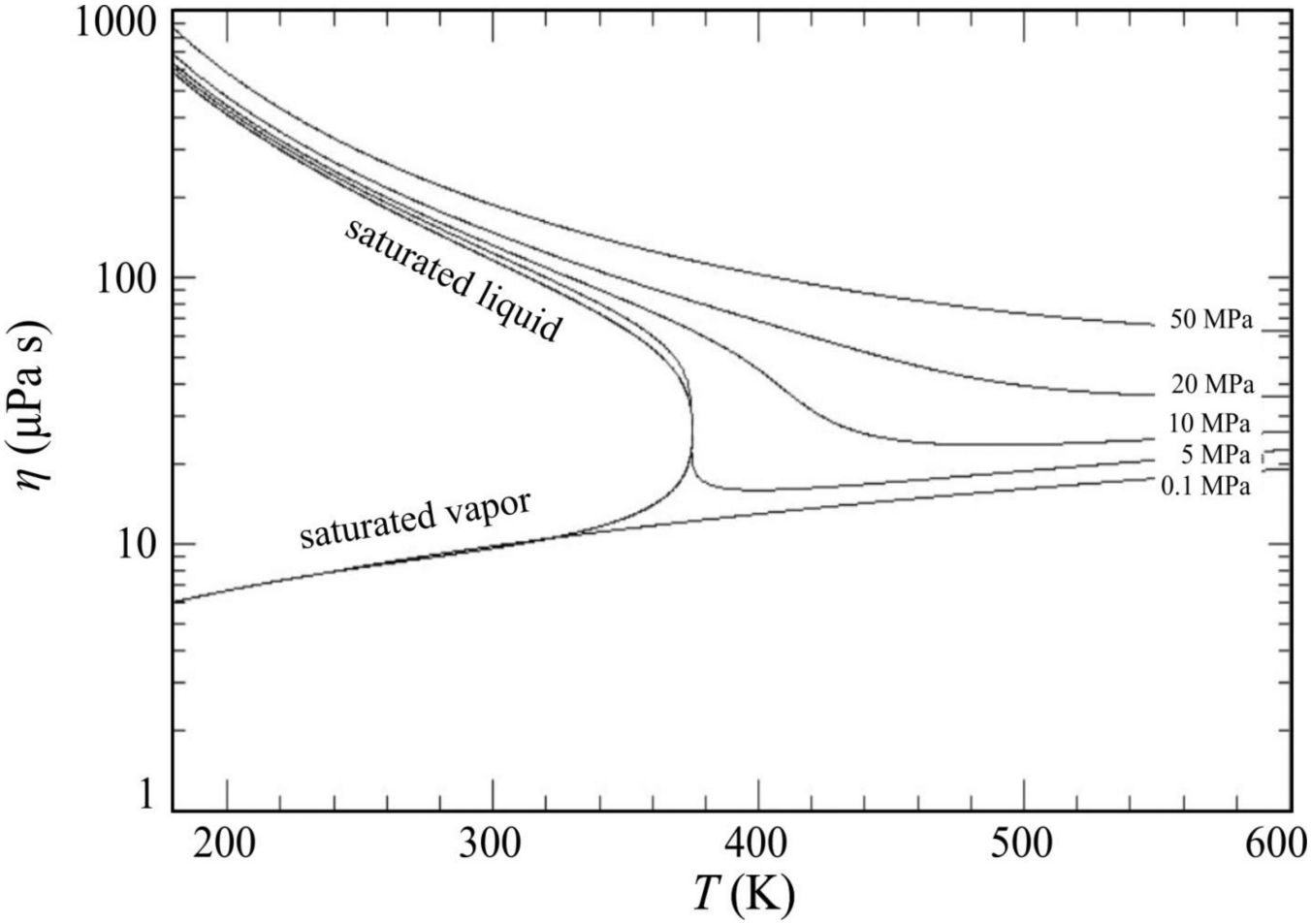

FIGURE 14.
Viscosity of R161 as a function of the temperature for different pressures.

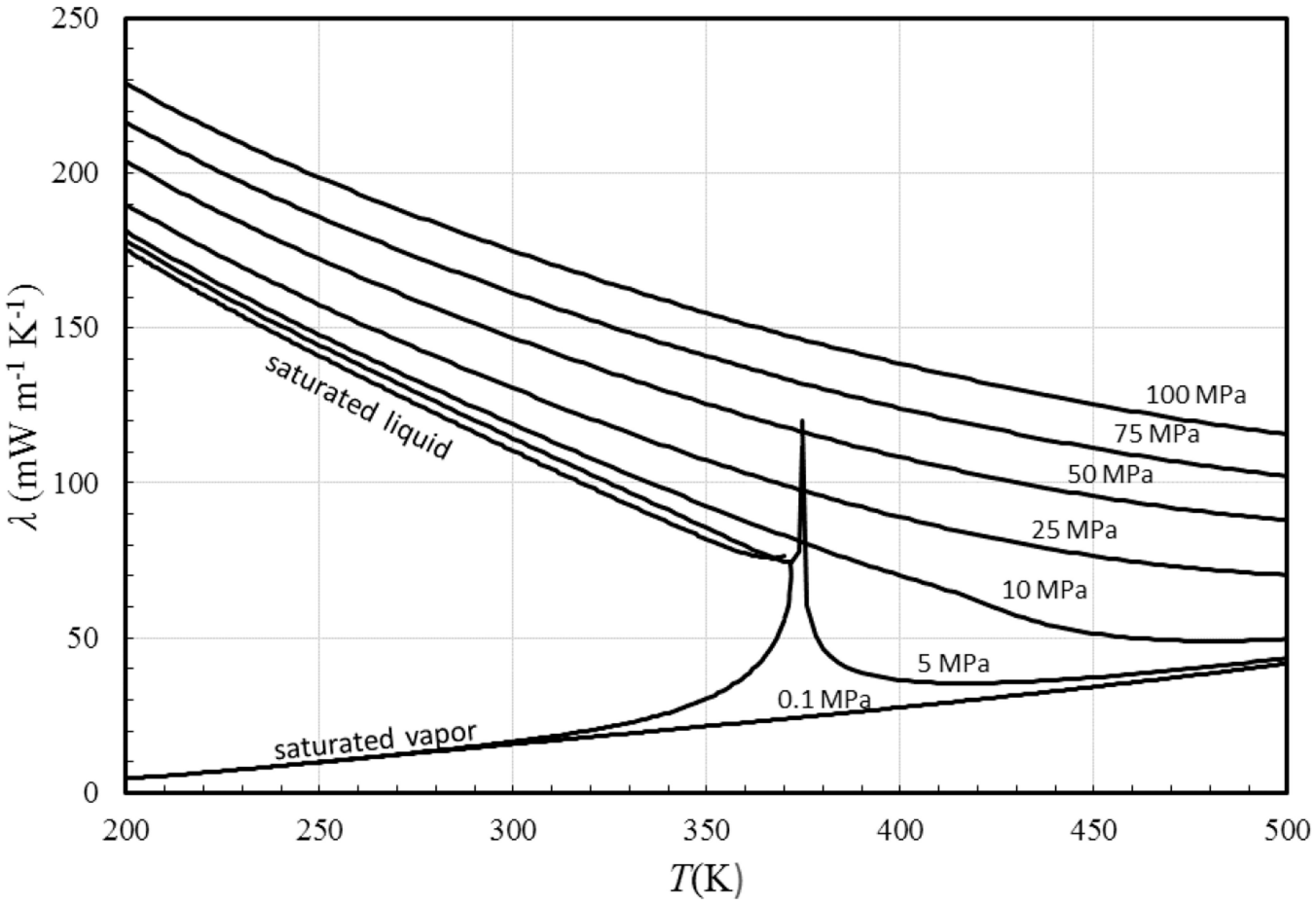

FIGURE 15.
Thermal conductivity of R161 as a function of temperature for selected pressures.

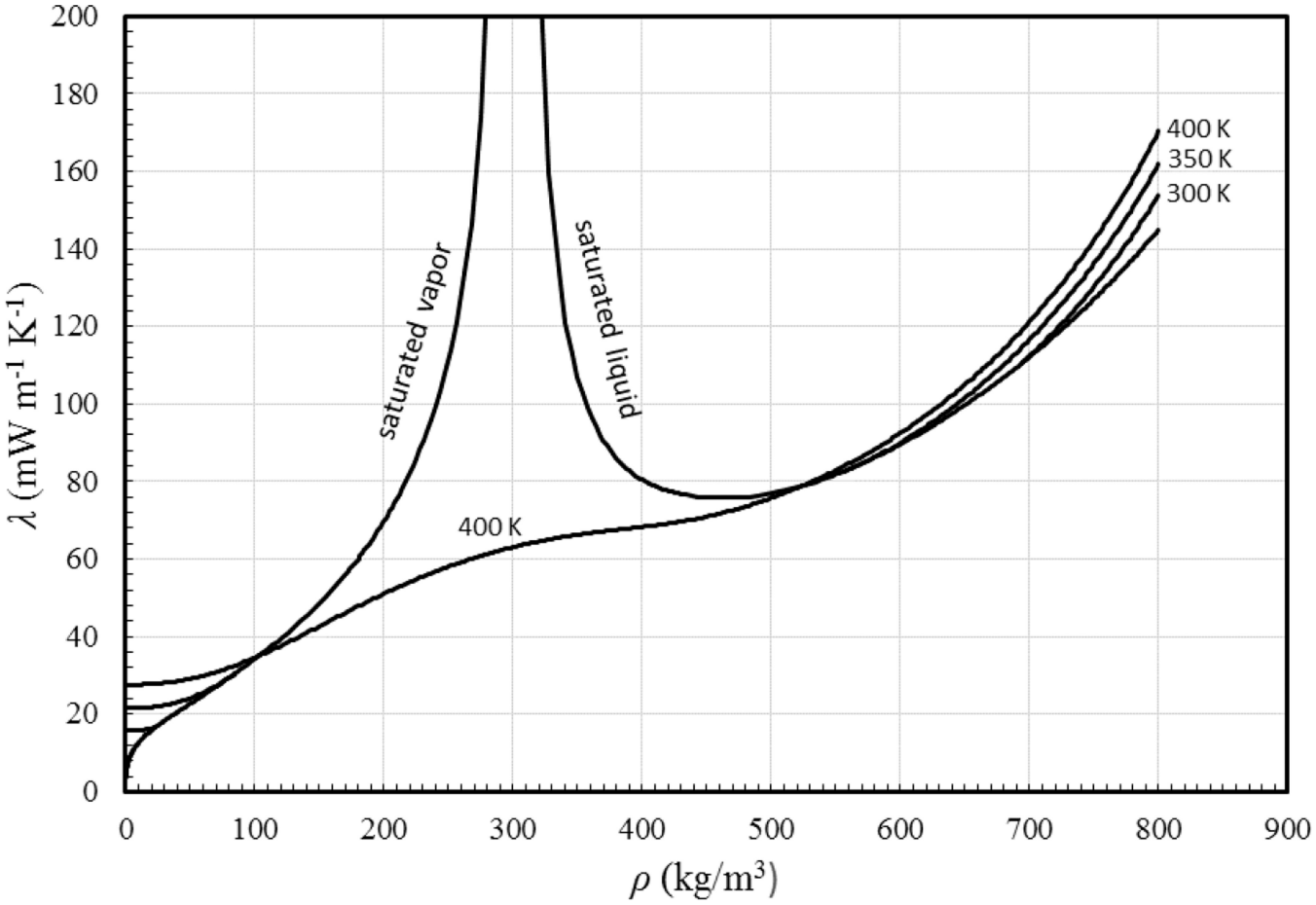

FIGURE 16.
Thermal conductivity of R161 as a function of density for selected temperatures.

TABLE 1

Viscosity measurements of R161

1st author	Year Publ.	Technique employed[a]	Purity (%)	Uncertainty (%)	No. of data	Temperature range (K)	Pressure range (MPa)
Bi[26]	2015	SLS	99.74	2	9	293–373	0.8–4.9
Meng[27]	2015	VB	99.74	3	91	243–363	0.1–30
Lv[28]	2014	OscD	99.95	1	24	293–370	0.1–0.5
Fan[29]	2012	Cap	99.95	3	29	233–371	0.09–4.7

[a]Cap, Capillary; OscD, Oscillating Disk; SLS, Surface Light Scattering; VB, Vibrating Wire.

TABLE 2

Coefficients and parameters for Eqs. (2), (3) – (7).

Molar mass	
48.0595 g/mol	
Scaling parameters	
ε/k_B = 320.39 K	σ = 0.4457 nm
Coefficients a_i for Eq. (3)	
a_0 = 0.241 30	a_1 = −0.450 00

TABLE 3

Coefficients b_i for Eq.(7)[30]

i	b_i
0	−19.572 881
1	219.739 99
2	−1015.322 6
3	2471.012 5
4	−3375.171 7
5	2491.659 7
6	−787.260 86
7	14.085 455
8	−0.346 641 58

TABLE 4

Coefficients c_i for Eq. (8).

i	c_i
0	−10.283 73
1	7.655 63
2	4.842 00
3	0.422 23
4	64.349 83
5	10.992 13

TABLE 5

Thermal conductivity measurements of R161

1st author	Year Publ.	Technique employed[a]	Purity (%)	Uncertainty (%)	No. of data	Temperature range (K)	Pressure range (MPa)
Wu[41]	2016	THW	99.74	1	117	234–373	0.9–20
Yao[42]	2014	THW	99.95	2–3	370	234–375	0.1–5.1

[a]THW, Transient Hot Wire.

TABLE 6

Coefficients of Eq. (15) for the residual thermal conductivity of R161.

i	$B_{1,i}$ (mW m^{-1} K^{-1})	$B_{2,i}$ (mW m^{-1} K^{-1})
1	−0.841 553×10^{1}	0.741 456×10^{1}
2	−0.397 744×10^{2}	0.440 586×10^{2}
3	0.106 179× 10^{3}	−0.819 833×10^{2}
4	−0.532 351×10^{2}	0.376 052×10^{2}
5	0.823 094×10^{1}	−0.490 293×10^{1}

TABLE 7

Evaluation of the R161 viscosity correlation for the primary data.

1st Author	Year Publ.	AAD (%)	BIAS (%)
Bi[26]	2015	1.44	0.17
Meng[27]	2015	0.55	−0.08
Lv[28],[a]	2014	0.55	−0.33
Fan[29]	2012	4.76	2.86
Entire data set		**0.95**	**0.52**

[a] pressures less than 0.5 MPa

TABLE 8

Evaluation of the R161 thermal-conductivity correlation for the primary data.

1st Author	Year Publ.	AAD (%)	BIAS (%)
Yao[42]	2014	1.67	−0.93
Wu[41]	2016	0.65	0.25
Entire primary data set		**1.39**	**−0.62**

TABLE 9

Viscosity and thermal conductivity values of R161 along the saturation line, calculated by the present scheme.

T (K)	p (MPa)	ρ_{liq} (kg m^{-3})	ρ_{vap} (kg m^{-3})	η_{liq} (μPa s)	η_{vap} (μPa s)	λ_{liq} (mW m^{-1} K^{-1})	λ_{vap} (mW m^{-1} K^{-1})
250	0.1880	789.54	4.64	204.34	8.15	140.98	9.92
275	0.4639	745.02	10.96	152.87	8.86	125.46	13.03
300	0.9716	693.43	22.76	115.89	9.64	110.40	16.56
325	1.8072	631.73	43.92	87.59	10.68	95.79	21.36
350	3.0880	551.03	84.51	63.78	12.54	81.95	30.41
375	5.0211	335.05	267.62	29.92	23.73	134.27	146.46

TABLE 10

Viscosity and thermal conductivity values of R161 at selected temperatures and pressures, calculated by the present scheme.

p (MPa)	T (K)	ρ (kg m^{-3})	η (μPa s)	λ (mW m^{-1} K^{-1})
10	250	803.6	223.3	147.9
	275	764.0	169.7	133.1
	300	719.8	131.8	118.9
	325	670.0	103.7	105.4
	350	612.6	81.80	92.7
20	250	815.9	242.0	154.3
	275	780.1	185.9	140.2
	300	741.5	147.1	126.9
	325	699.9	118.9	114.5
	350	655.4	97.86	103.0

TABLE 11

Sample points for computer verification of the correlating equations.

T (K)	ρ (kg m^{-3})	η (μ Pa s)	λ (mW m^{-1} K^{-1})
250	0	8.280	9.892
250	1	8.255	9.884
250	850	308.22	175.48
375	0	12.171	24.517
375	229	20.859	81.297
375	229	20.859	32.433[a]

[a]Calculated with critical enhancement set to zero